Geophysics Open-File Report 7a
Geoscience Department
New Mexico Tech
Socorro, NM 87801

THE RELATIONSHIP OF MICROEARTHQUAKE ACTIVITY TO STRUCTURAL GEOLOGY FOR THE REGION AROUND SOCORRO, NEW MEXICO

by

Richard P. Mott, Jr.

Submitted in partial
fulfillment
of
the requirement
of
Geophysics 590
and the
Master's Degree Program
at
New Mexico Institute
of
Mining and Technology

May, 1976

The research described in this paper was sponsored jointly by the National Science Foundation (DES74-24187) and the State of New Mexico (Board of Educational Finance (BEF-6) and Energy Resource Board (ERB-75-300)).

ABSTRACT

An eight-month survey of microearthquake activity in the region around Socorro, New Mexico has been made using portable high-magnification (5 million at $60H_Z$) seismographs. In all 359 microearthquakes have been located which, because of multiple events and swarms, can be represented by 88 separate epicenters. Focal depths for the 298 most accurately located shocks indicate that microearthquakes occur from 0.0 to 14.0 km beneath the surface but two-thirds of all foci are concentrated at depths between 6.0 and 9.0 km. Epicenters are concentrated in a zone along the axis of the Rio Grande rift. Within the seismicly active zone, epicenters are diffuse and in general cannot be associated with known faults. From three composite fault-plane solutions, normal faulting is indicated along a north-northeast plane. The solutions also indicate a near-horizontal, west-northwest-trending axis of least principal (tensional) stress which agrees with the east-west tensional tectonic regime frequently suggested for the Rio Grande rift.

Microearthquake swarms have been studied because of their frequent association with magmatic processes. Swarms are found to be confined to the area around Socorro Mountain. This observation supports other geophysical and geological evidence that indicates recent or current magmatism beneath Socorro Mountain. Analysis of S_XS reflection phases generated

by microearthquakes has been used to further map the magma layer at 18 km depth beneath Socorro. Reflection points indicate the magma layer is 4 km wider in the east-west direction, extends 3.5 km further south, and has an overall more northerly trend than had been previously reported. Evidence indicates the southeast boundary of the magma layer may occur beneath Socorro. Analysis of the depth at which the reflections occur shows the average reflection occurs at 20 km but that there may be regional variations in the depth to magma surface. The location of microearthquake activity appears to be unrelated to the presence or absence of the magma layer.

INTRODUCTION

Microearthquakes, earthquakes with M_L 2?, have been shown to occur frequently near Socorro, New Mexico in numerous publications. Sanford et al. (1972) suggested that the most seismically active portion of the Rio Grande rift may occur between Socorro and Bernardo, New Mexico. The region around Socorro has both Recent faulting (Sanford et al., 1972) and Late Tertiary-Quaternary volcanic activity (Bruning, 1973). Thus both volcanic and faulting processes are possible sources of microearthquake activity.

The purpose of this report is to discuss the results of an eight-month survey of microearthquake activity in the Socorro region. In particular, this report explores the relationship between microearthquake activity and 1) major structural features, 2) faulting, 3) volcanic and magmatic processes, and 4) the occurrence of a magma layer at a 18 km depth beneath Socorro. The report is divided into 5 sections: 1) previous geophysical studies, 2) previous geological studies, 3) instrumentation, 4) location procedure, and 5) results and conslusions.

GEOLOGIC SETTING

Rio Grande Rift

Socorro lies within the Rio Grande depression (see Figure 1), a major continental rift extending 1000 km between Leadville, Colorado and El Paso, Texas (Chapin, 1971). Rifting began approximately 29 m.y.a. although the rift itself is superimposed on a tectonic belt which had previously undergone deformations during the late Paleozoic and Laramide (Chapin and Seager, 1975). Basin-and-Range type faulting characterizes the rift and has produced a series of basins and mountain ranges arranged en echelon with a general north trend.

Geology of the Socorro Region

Near Socorro, the Rio Grande rift is expressed as north-trending elevated blocks separated by structural basins (see Figure 2)(Sanford et al., 1972). From east to west, the structurally elevated areas are (1) La Joyita Hills, (2) Ladron, Socorro-Lemitar, and Chupadera Mountains, and (3) the Bear and Magdalena Mountains. Separating these features are the Socorro and La Jencia basins. A major northeast-trending structural low is the San Augustin lineament which separates both the Ladron and Socorro-Lemitar Mountains (Woodward, 1973) and the Bear and Magdalena Mountains (Chapin, 1971). Similarly a minor east-trending graben or volcanic collapse feature separates the Socorro-

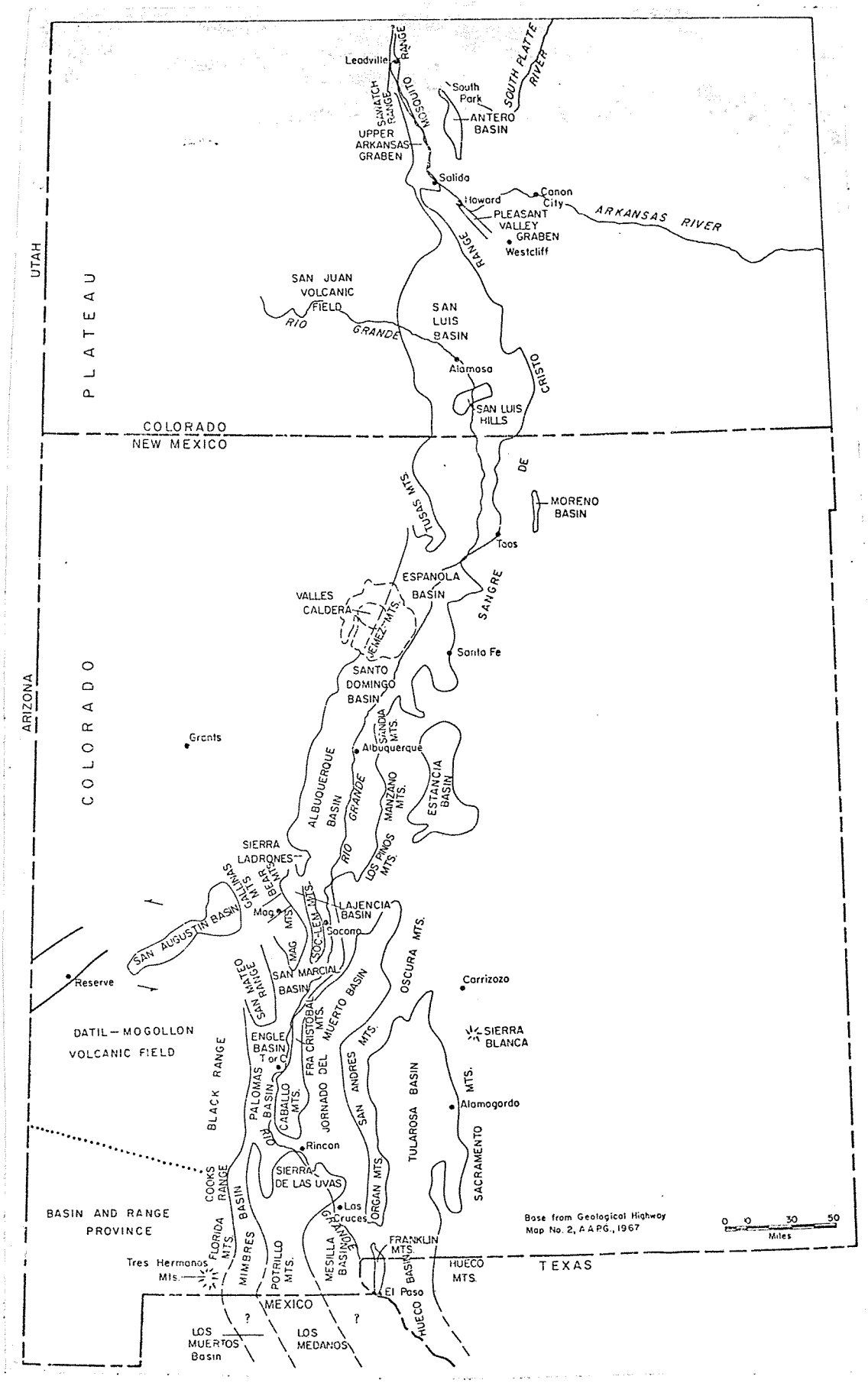

Figure 1. Generalized map of the Rio Grande rift (after Chapin, 1971).

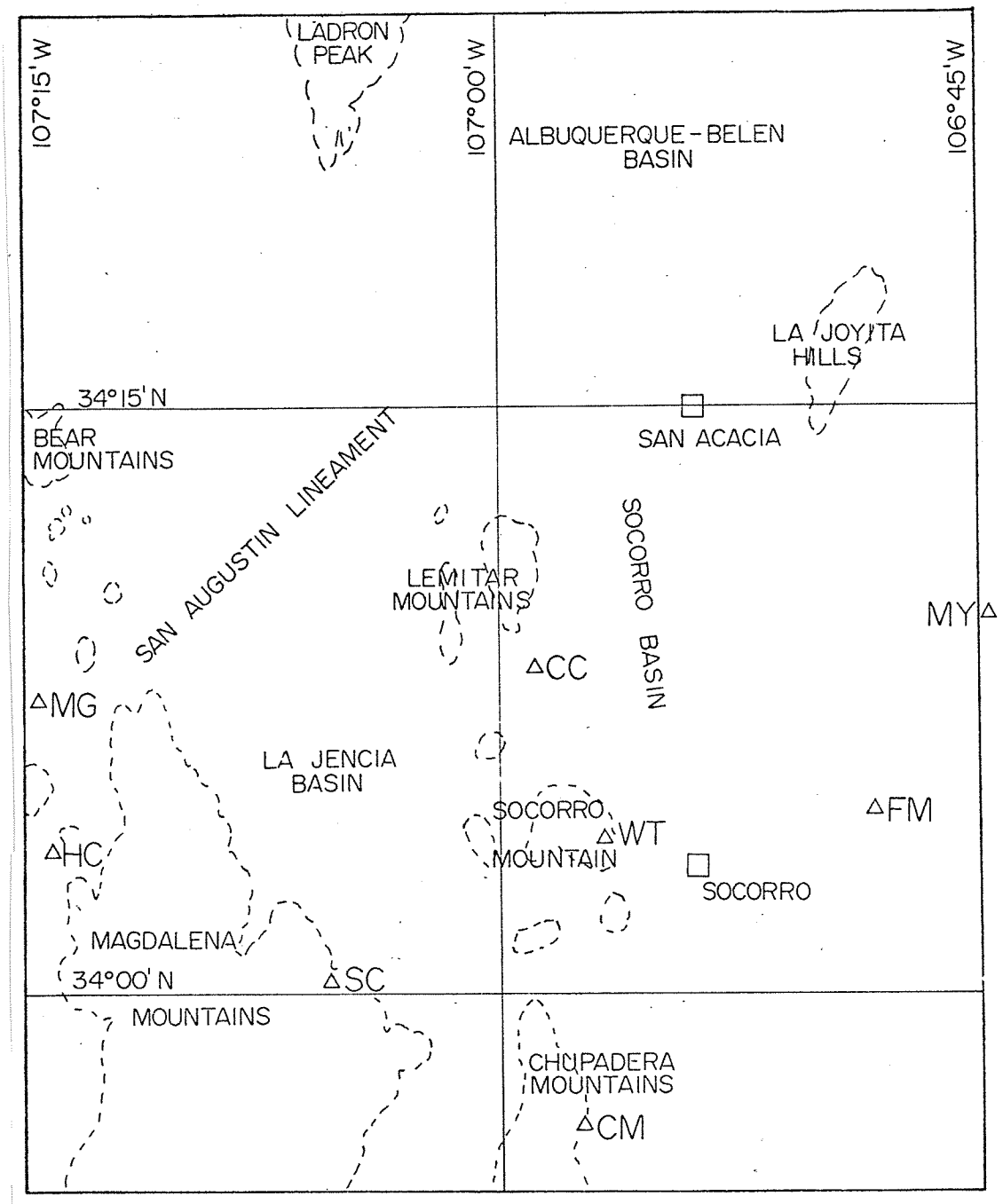

Figure 2. Map of the major structural features and seismograph stations nearest to Socorro. Stations were occupied between April 15 and December 15, 1975.

Lemitar and Chupadera Mountains (Sanford, 1968).

Structural Highlands

La Joyita Hills are a north-trending and west-dipping horst. The eastern section of the horst is a Precambrian gneiss complex and the western section outcrops post-Mississippian sedimentary rocks (Herber, 1963). Evidence from the depositional contact between the sedimentary rock and the gneiss indicates that they reacted as a single unit during westward tilting (Herber, 1963). Major normal faults bound La Joyita Hills on the east and west and have north and northeast orientations respectively. Less continuous east-trending normal faults are present throughout the horst (Herber, 1963).

The Ladron Mountains are predominantly an uplifted block of Precambrian rock with lesser amounts of Paleozoic sedimentary rocks outcroping in their western and southern extent. The large exposures of Precambrian rock suggest that the Ladron Mountains are structurally higher than the Socorro-Lemitar and Chupadera Mountains to the south (Sanford et al., 1972). The Ladron Mountains have undergone several cycles of uplift and erosion with the last major episode occurring during the late Miocene and/or Pliocene (Chapin and Seager, 1975). A series of north-trending faults have been produced throughout the mountains and a lesser pattern of northeast-trending faults have developed where the Ladron Mountains intersect the San Augustin lineament.

The Socorro-Lemitar Mountains are a west-dipping intra-graben horst which was uplifted sometime after 9-10 m.y.a. (Chapin and Seager, 1975). Chapin and Seager (1975) suggest that this structure may have formed by thin-skinned extention similar to that described by Anderson (1971) for southeastern Nevada. Along the eastern side of the mountains, Precambrian rock outcrops extensively but progressively lessens in extent southward. Widespread outcrops of Miocene-aged Popotosa Formation are exposed in the western and southern sections of the mountains (Woodward, 1973; Bruning, 1973). The Popotosa Formation is an early-rift basin deposit (predating the Socorro-Lemitar Mountains) composed of playa and fanglomerate facies with lesser amounts of andesitic volcanics (Bruning, 1973). Faulting within the Socorro-Lemitar Mountains has both a north and east pattern. It is predominatly high-angle normal and reverse in character and thus has created a series of uplifted and rotated blocks (Woodward, 1973). The southern end of the Socorro-Lemitar Mountains is composed of volcanic and intrusive rocks dated 10-12 m.y.b.p. (Burke et al., 1963; Willard, 1971). Chapin and Chamberlin (personal communication) suggest that the igneous complex is the northern border of the remanence of a volcanic caldera.

The Chupadera Mountains are an uplifted block of predominantly mid-Tertiary volcanics, specifically the Datil Formation (Dane and Bachman, 1965). In the north end of the mountains, minor exposures of volcanics dated 10-12 m.y.b.p. outcrop and are presumably related to the igneous rocks in

the south end of Socorro Mountain (Willard, 1971). In the southern Chupadera Mountains, large outcrops of Precambrian and Paleozoic rock have been interpreted as indicating that this area has been preferentially uplifted. This uplift has created several major east-trending normal faults. Bounding faults of the Chupadera Mountains are normal and north-trending.

The Bear Mountains consist of mid-Tertiary rhyolites and andesites forming a north-trending west-dipping hogback (Brown, 1972). The lack of mature dissection, characteristic of other local ranges, has been interpreted by Chapin and Seager (1975) as indicating the Bear Mountains are the youngest uplift in the Socorro vicinity. Faulting throughout the mountains is north-trending except where the Bear Mountains intersect the San Augustin lineament (Brown, 1972). At this intersection, faulting is northest-trending with minor amounts of oblique slip (Chapin, 1971).

The area of the Magdalena Mountains has been actively faulted and uplifted since Laramide time (Bruning, 1973). Currently the north end of the range is composed of major outcrops of Precambrian and Pdleozoic rocks and lesser outcrops of Tertiary intrusives and volcanics. In the central and southern regions, Tertiary volcanics compose the majority of outcrops. The relative differences in bedrock ages and stratigraphic positions indicate the northern section of the mountains has been preferentially uplifted (Sanford et al., 1972). Four major fault trends have formed in the Magdalena

Mountains since Oligocene time (Chapin et al., in preparation). They are 1) a west-northwest system of transverse faults (Oligocene), 2) a north-northwest pattern of extensional faults (circa 28 m.y.a.), 3) a north-trending series of normal faults related to Basin-and-Range deformation (Miocene), and 4) a northeast-trending system of faults related to the development of the San Augustin lineament (less than 14 m.y.a.). The most recent volcanic eruptions in the Magdalena Mountains are rhyolitic flows which emanated from the Magdalena Peak dome 14 m.y.a. (Weber and Bassett, 1963).

Basins

The Socorro and La Jencia basins are similar in structure and depositional history and thus can be discussed together. Both basins are filled with a thick sequence of Santa Fe sediments which obscures older rocks and deep structures. The thickness of fill, estimated from gravity data is approximately 900 meters in Socorro basin and 450 meters in La Jencia basin (Sanford, 1968). (Further structural implications from gravity data will be discussed in the section of this study dealing with geophysical investigations.) Playa and fanglomerate facies compose the majority of basin sediments with lesser amounts of andesitic and basaltic flows. The most recent exposure of volcanics in either basin occurs near San Acacia and is an andesitic basalt of Late Tertiary or Quaternary age (Bruning, 1973).

Faulting within the Socorro and La Jencia basins has a predominant north-trend and dip angles which range from 70-90° (Sanford et al., 1972). A second pattern of east-trending faults are also present but are shorter and more widely spaced (Sanford et al., 1972). The north-trending faults within the Socorro basin are not consistently down-thrown towards the Rio Grande and thus horsts occur within the broader basin-valley structure. The Socorro-Lemitar Mountains are an excellent example of these intragraben horsts. North-trending Quaternary faults within the Rio Grande-rift basins tend to be discontinuous, with individual faults being traceable for only several kilometers (Sanford et al., 1972). Within both basins, zones of closely spaced parallel faults are separated by large areas of ground not affected by faulting (Sanford et al., 1972). The most intense Quaternary faulting within the rift extends from San Acacia to San Antonio in the Socorro basin (Sanford et al., 1972). The greater part of La Jencia basin is relatively unaffected by Quaternary faulting.

Extensive geomorphic surfaces of Quaternary age have developed in the Socorro and La Jencia basins. Four of these remanent pediments are described by Denny (1941) and appear below with their projected grades above the present Rio Grande flood plain.

Ortiz pediment	112.8-121.8 meters
Tio Bartolo pediment	76.2 meters
Valle de Parida pediment	45.7 meters
Cañada Mariana pediment	15.2-22.9 meters

Several major faults displace these surfaces by as much as 15 meters verifying that recent tectonism has occurred in the Socorro area (Sanford et al., 1972).

The San Augustin lineament is a northeast-trending downdropped block filled with Santa Fe sediments. In the Magdalena area, bounding faults are left-lateral oblique-slip in character and have 0.8-1.5 meters of displacement (Chapin, 1971). Chapin (1975) has suggested that the San Augustin lineament represents a bifurcation of the Rio Grande rift and was formed during the Late Miocene and/or Pliocene.

The structural low between the Socorro-Lemitar and Chupadera Mountains is small in area but may be geologically important. On the surface are Late Tertiary and/or Quaternary aged andesitic basalt flows which are possibly the most recent volcanics in the Socorro area (Bruning, 1973). As discussed previously, this structural low was suggested by Sanford (1968) to be the area of a volcanic collapse feature and has more recently been proposed by Chapin and Chamberlin (personal conversation) to be the northern extent of a volcanic caldera.

PREVIOUS GEOPHYSICAL INVESTIGATIONS IN THE SOCORRO AREA

Geographic Distribution of Microearthquake Activity

Investigation of microearthquake activity in the vicinity of Socorro began in 1960. Results of the studies are described by Sanford and Holmes (1961, 1962), Sanford (1963), Sanford and Long (1965), Sanford and Singh (1968), Singh (1970), Sanford et al. (1972), and Sanford et al. (1973). Conclusions reached in these studies that relate to the geographic distribution of microearthquake activity are discussed below.

The number of microearthquakes with M_L greater than 0 occurring within a 20 km radius of Socorro averages around 400 per year. Most microearthquakes are located to the west and southwest of Socorro (Figures 3,4,5) and also in an area separating the Albuquerque-Belen and Socorro basins near San Acacia (Figure 5). The Socorro basin itself appears to be aseismic. The relationship between seismic zones and known geologic sturcture is not obvious. Activity appears to be unrelated to known faults or fault-defined margins between highlands and basins (Sanford, 1968; Sanford et al., 1972). The events occurring to the west and southwest of Socorro are possibly related to recent igneous intrusives or to current magmatic action at depth (Sanford, 1963).

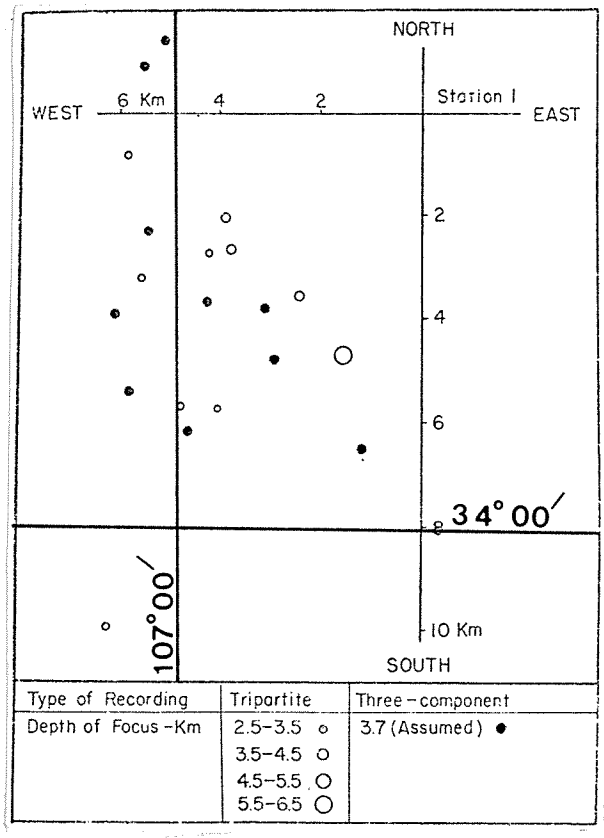

Figure 3. Geographical distribution of microearthquakes near Socorro from July, 1960 to July, 1961 (after Sanford and Holmes, 1962).

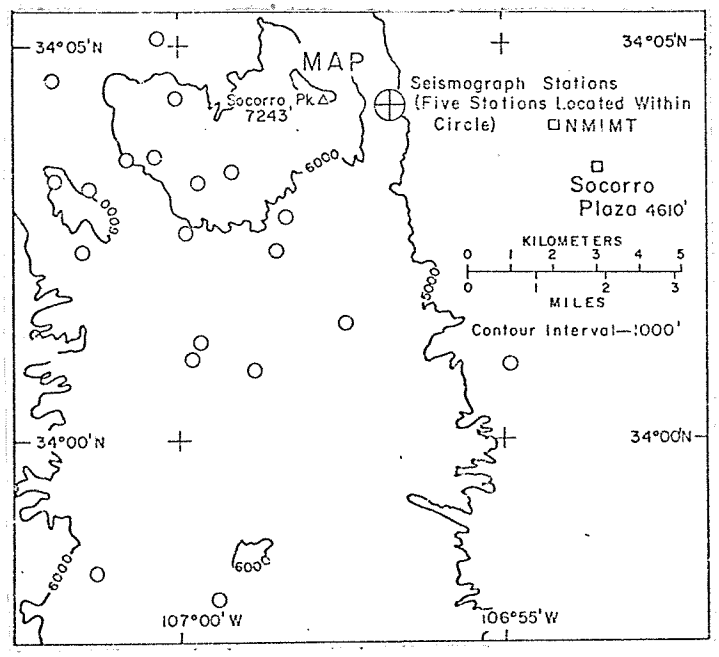

Figure 4. Map showing the location of weak earthquakes which occurred near Socorro from Sept., 1960 through Jan., 1961 and from Nov., 1962 through Dec., 1962 (after Sanford, 1963).

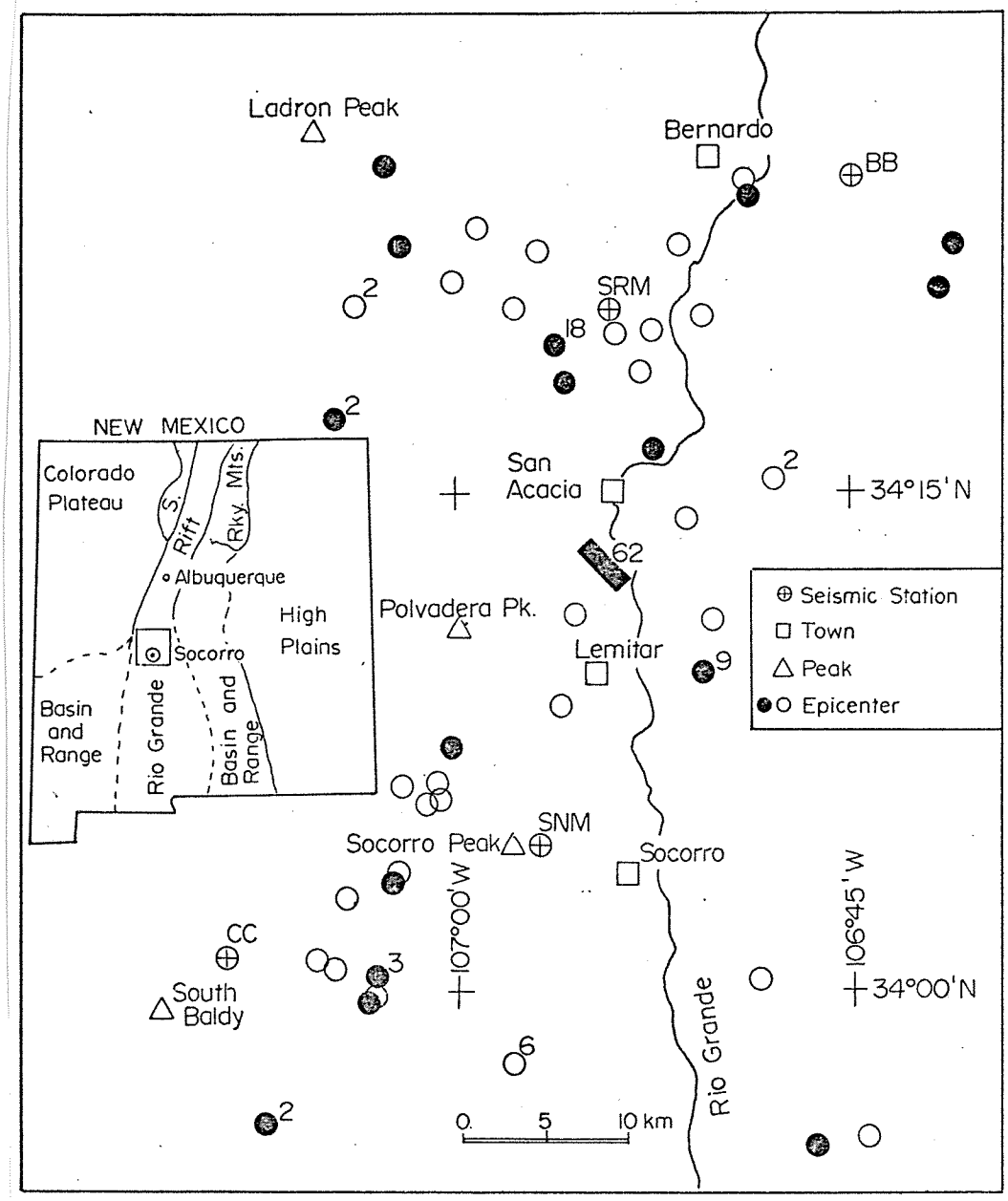

Figure 5. Locations of epicenters in the Bernardo to Socorro segment of the Rio Grande rift from July 1, 1969 through June 30, 1970. The solid circles and rectangle indicate good earthquake locations; open circles indicate fair locations. Numbers are used when more than one event occurs at a given location (from Sanford et al., 1973).

Microearthquake Phases Reflected Off A Discontinuity At Approximately 18 km

The use of microearthquake reflected phases to study the seismic velocity discontinuity at 18 km beneath the Rio Grande rift is described by Sanford and Long (1965) and Sanford et al. (1973). In the research described in these papers, the discontinuity was found to be at a depth of 18 km directly beneath Socorro and to dip northward to a depth of 30 km, at a distance of 60 km north of Socorro. The minimal area underlain by the discontinuity is delineated by the reflection points in Figure 6.

Gravity Investigations

Two detailed studies of the gravity of the Rio Grande rift near Socorro have been made by Anderson (1955) and Sanford (1968). A series of residual Bouguer anomaly maps by Sanford (1968) define major elongate gravity lows extending north-south (Figures 7,8,9). These lows are the gravitational expression of the Socorro basin and La Jensia basin. A close spacing of gravity contours indicates that the Socorro basin is bounded on the west (along the east edge of Socorro Mountain) by a narrow fault zone with a large displacement (Sanford, 1968). The eastern boundary of the basin has a wide contour spacing which suggests step-faulting in this area. Thus the Socorro basin is asymmetric being sharply downthrown to the west. La Jencia basin is everywhere bounded by widely spaced gravity contours suggesting that step-faulting and

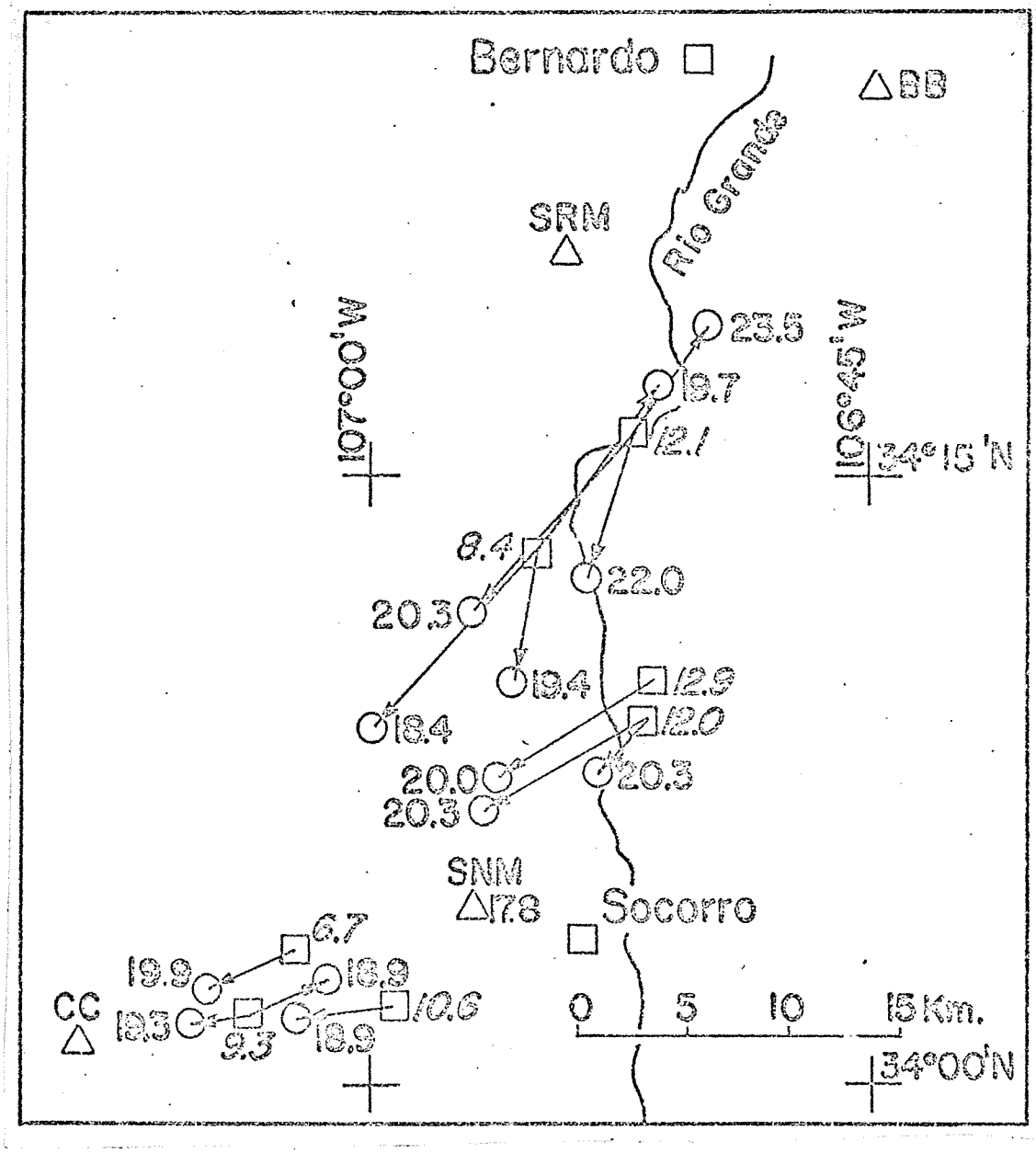

Figure 6. Map showing depth of the discontinuity in the vicinity of Socorro. Discontinuity depths are given at the reflection points (circles) and focal depths are given at the epicenters (squares) (after Sanford et al., 1973).

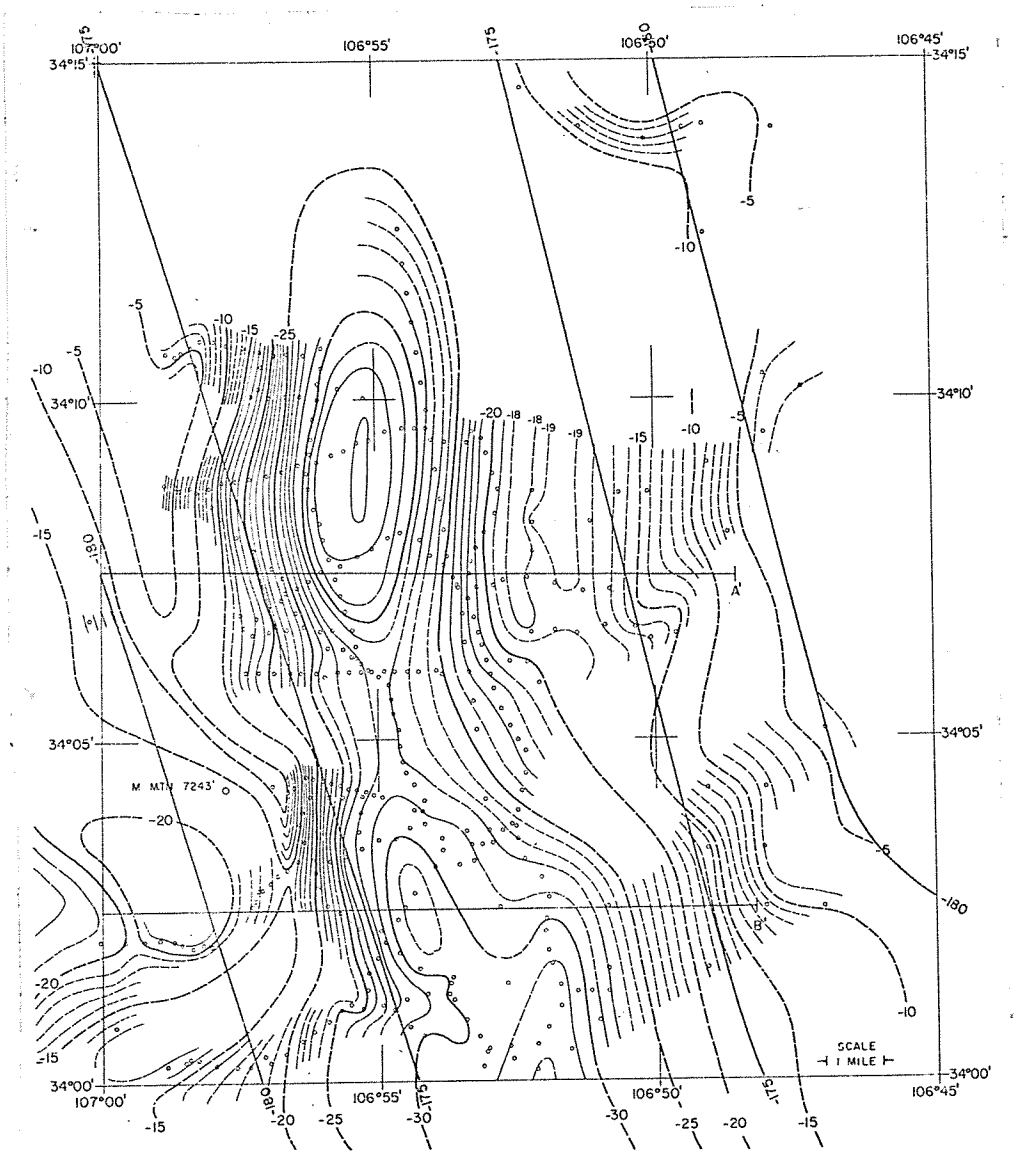

Figure 7. Residual Bouguer anomaly map for the Socorro quadrangle (after Sanford, 1968).

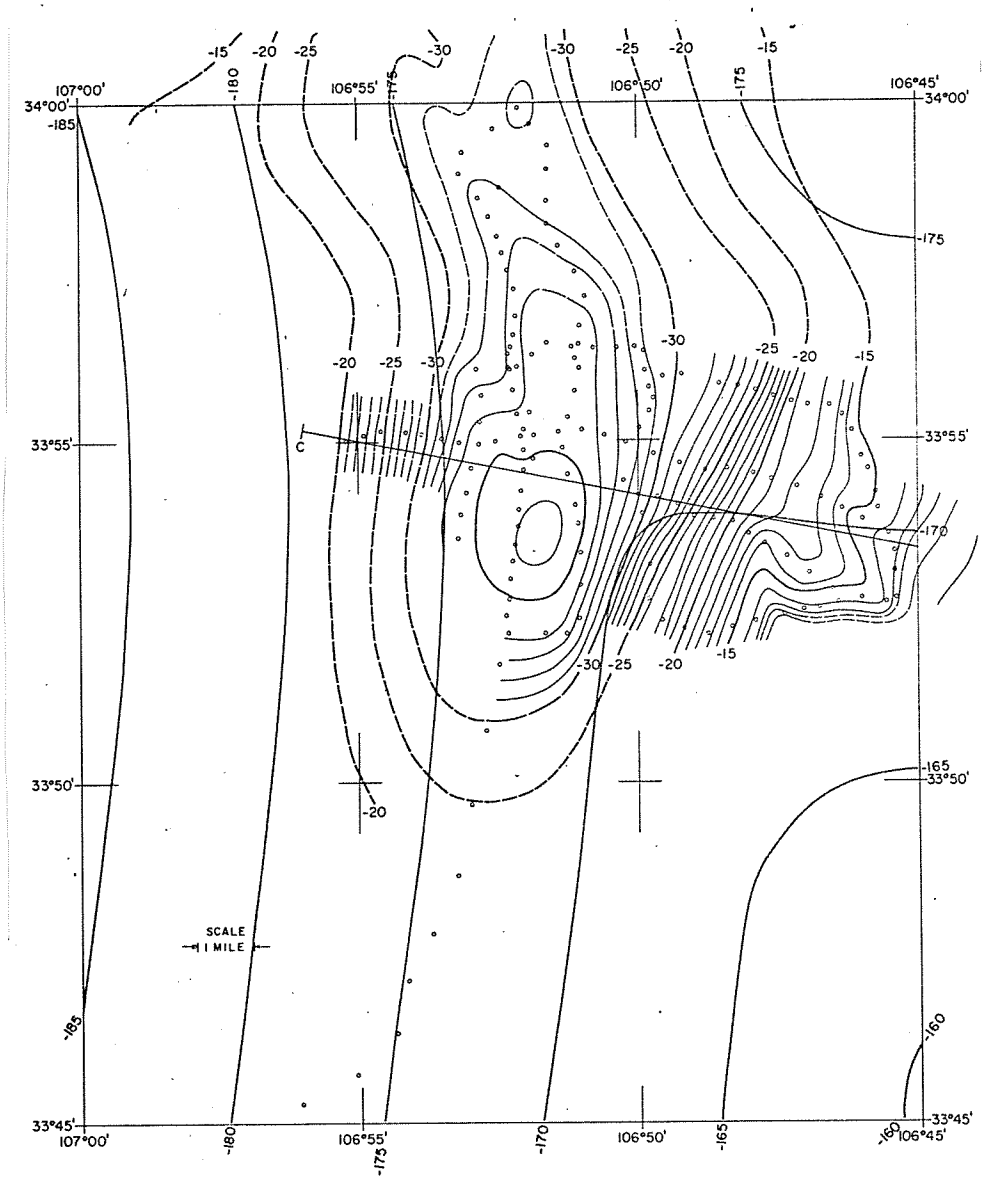

Figure 8. Residual Bouguer anomaly map for the San Antonio quadrangle (after Sanford, 1968).

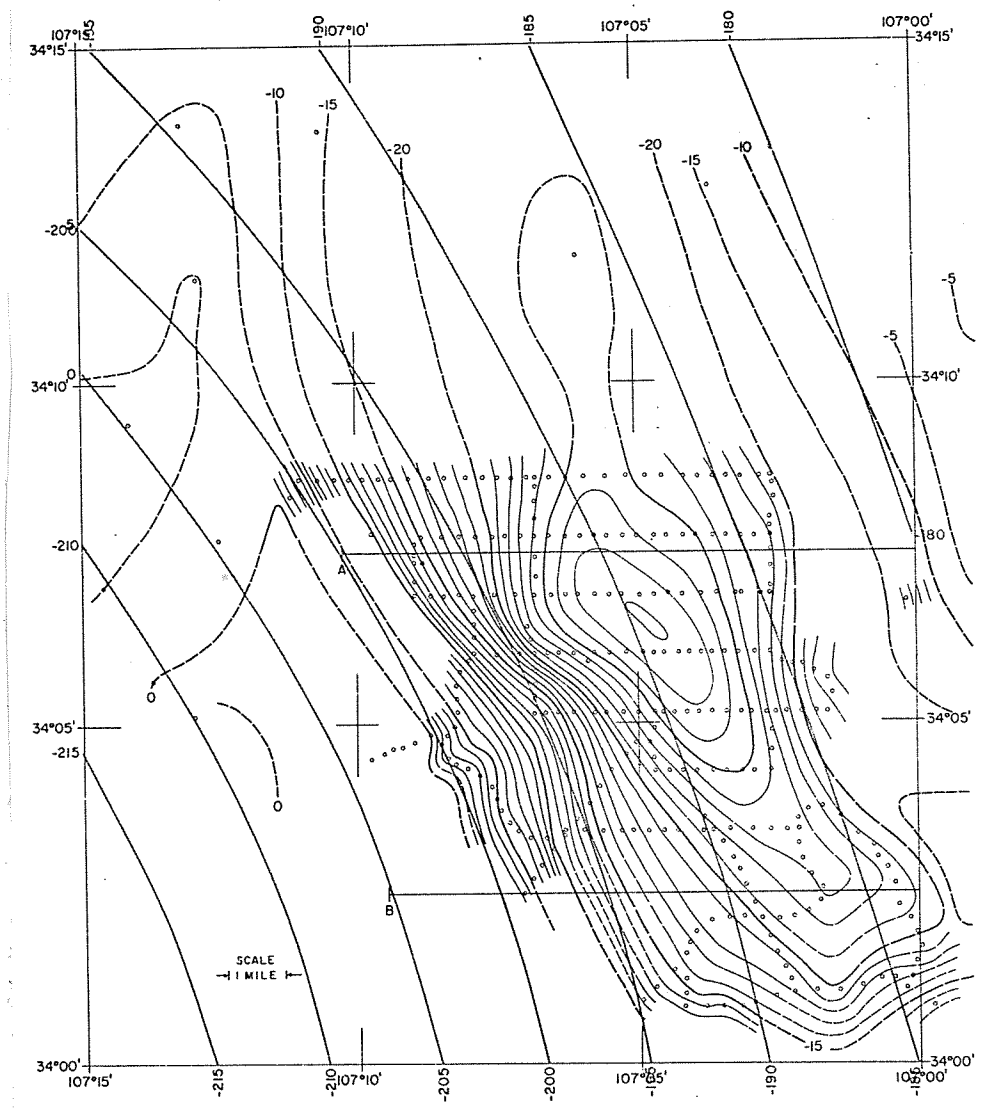

Figure 9. Residual Bouguer anomaly map for the Magdalena quadrangle (after Sanford, 1968).

tilting occurs over a broad zone from the mountain fronts to the center of the depression. In the previously defined seismic area near the southwest end of Socorro Mountain, a semicircular structural high surrounding a circular structural low (Figure 7) is indicated by the Bouguer residuals. This is interpreted by Sanford (1968) as a volcanic collapse feature related to the recent intrusives in the Socorro Mountains.

Magnetic Studies

Aeromagnetic maps constructed by the New Mexico Bureau of Mines and Mineral Resources (in cooperation with the U. S. G. S.) and a detailed study of the southern end of Socorro Mountain by Ramananantoandro (1965) constitute the only magnetic investigations in the Socorro vicinity. The aeromagnetic maps are constructed from total field measurements and are displayed as residual magnetic intensities. Broad widely-contoured residual lows, trending north, characterize the Socorro basin and La Jencia basin. Closely-contoured nodes of alternating high and low residuals are representative of the Magdalena and Lemitar Mountains. Southwest of Socorro Mountain, in the area previously discussed as a seismic zone and a gravity low, there exists a low magnetic residual of approximately the same value as the residual associated with Socorro basin. It is the author's opinion that this further indicates the presence of a collapse feature (i.e. a graben or caldera). For the same area, a

low magnetic residual, of smaller lateral dimensions, is mapped by the vertical component measurements of Ramananantoandro (1965). A series of high magnetic residuals are also mapped south and west of Socorro Mountain which are concluded to be associated with intrusions and flows of basic rocks.

Terrestrial Heat Flow Investigations

Evidence for an anomalously high heat flow in the Socorro area is discussed by Hall (1963), Summers (1965), Reiter et al. (1975), and Sanford and Reiter (manuscript in preparation). Regionally, a ribbon of high heat flow is found to exist along the western side of the Rio Grande rift (Reiter et al., 1975). Within 40 kilometers of Socorro, five heat flow measurements are reported. Four range between 1.9 and 2.8 H.F.U. (heat flow units) (Reiter et al., 1975). The fifth measurement, made within a mine in Socorro Mountain, has an especially high heat flow of 11.5 H.F.U. (Sanford and Reiter, manuscript in preparation). Six thermal springs and wells (68-91°F.) along the east face of Socorro Mountain and three thermal springs (approx. 70°F) in the vicinity of San Acacia (Hall, 1963; Summers, 1965) present further evidence for a locally-high terrestrial heat flow.

INSTRUMENTATION

Four to six Sprengnether Instrument Company MEQ-800 portable seismic systems composed the primary equipment used to record microearthquakes in this study. Each system consisted of either a Mark Products L4C (1.0 Hz) or a Willmore (1.5 Hz) vertical seismometer, a gain-stable amplifier, a quartz-crystal-controlled timing system, and a smoked-paper recorder. Gain settings could be varied from 60dB to 120dB by 6dB steps and were set according to background noise conditions. Filtering of low and high frequency signals was possible but only filtering of signals above 30 Hz, on particularly windy days, was ever used.

A plot of the magnification vs. frequency is shown in Figure 10 for the MEQ-800 seismic systems operating at typical gain and filtering settings. The magnification peaks near 5×10^6 for a frequency around 60 Hz. The high magnification at high frequencies makes the MEQ-800 seismic system excellent for studying microearthquakes which are characterized by small ground displacements and high frequencies.

Clocks in all the seismic systems were synchronized to WWV-UST at the onset of each recording "week" (3-5 days). The clocks were similarly checked for drift at the completion of each recording period. Drifts ranged from 0.00 to 0.30 seconds per recording "week" with most units showing

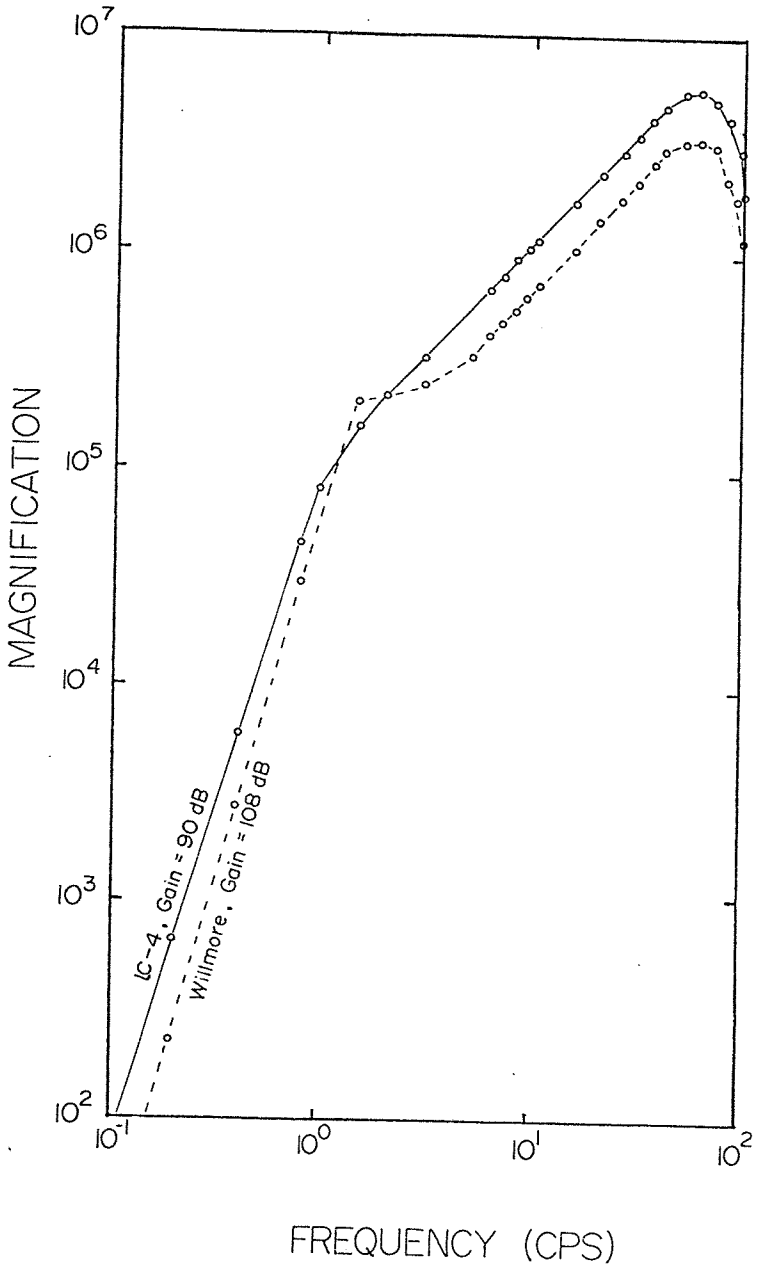

Figure 10. Graph of the magnification versus frequency for for an MEQ 800 seismic system and either a L4-C or Willmore geophone. The gain for the L4-C and Willmore systems is set for standard operating conditions, 90dB and 108dB. The filter settings for both systems are also set for standard operating conditions, high filter-out and low filter-out.

drifts less than 0.15 seconds. When timing corrections were calculated, time drifts were assumed to occur linearly. At the recording speed of 120 mm/minute, P-arrival times could be read to within ±0.035 seconds (0.07 mm). Because of differences in the sharpness of S-phase arrivals, the accuracy in timing S-P intervals varied greatly. As an estimate, the accuracy was probably on the order of ±0.1 second.

During the course of this survey, nine recording stations were occupied. Locations for the eight stations nearest to Socorro are shown in Figure 2 and location parameters for every station are listed in Table 1. All stations were located on consolidated sedimentary or igneous rock in order to avoid arrival-time delays and corresponding station-related timing corrections. Analysis of arrivals from natural shocks and explosions demonstrated that corrections of this type were not necessary.

Table 1. Seismic Station Location Parameters

Station	Latitude	Longitude	Elevation(m)	Rock Type	Age
CC	34.1442	106.9812	1510	metasediment	Precambrian
CM	33.9501	106.9579	1640	ashflow tuff	mid-Tertiary
FM	34.0829	106.8047	1573	metasediment	Precambrian
HC	34.0658	107.2361	2240	rhyolite, Santa Fe Gp.	Miocene
MG	34.1305	107.2425	2024	felsic volcanics	Tertiary
MY	34.1667	106.7459	1645	sandstone, Yeso Fm.	Permian
NJ	33.9924	106.6254	1644	Mancos Shale	Cretaceous
SC	34.0100	107.0894	2073	rhyolite, Datil Gp.	mid-Tertiary
WT	34.0722	106.9459	1564	igneous	Precambrian

LOCATION PROCEDURE

For the purpose of locating microearthquakes, the crust near Socorro was assumed to be a homogeneous half-space with a P-wave velocity of 5.8 km/sec. Initially, microearthquakes were located by a computer adaptation of the standard graphical technique which uses the intersection of chords (representing the intersection of hemispheres). These locations were later checked by using the same data in an iterative numerical location program. The agreement between locations determined by both methods was excellent. In both techniques, the S-P interval was utilized to assist in determining an approximate origin time. Origin times were calculated from the following equation

$$\text{Origin Time} = P - \frac{S - P}{V_p/V_s - 1.0} \quad ,$$

where, P and S are the arrival times and V_p and V_s are the velocities, for the P and S waves. In this study, Poisson's ratio was assumed to be 0.25 and therefore V_p/V_s reduced to $\sqrt{3}$. The origin time equation thus became

$$\text{Origin Time} = P - (S - P)(1.3666) \quad .$$

Microearthquake locations determined in this study were catagorized as Class A or Class B according to their accuracy. The absolute accuracy of either class of events is difficult to estimate. Epicenters may be systematically shifted in

particular regions because the crustal structure assumed for location procedures may deviate substantially from the true structure. The relative locations for Class A events are quite good being within ±0.5 km in geographic location and ±2.0 km in depth. Locations were classified as B for any one of the following reasons:

1.) The epicenter was outside the seismic-station array.

2.) The microearthquake was recorded at only three stations.

3.) Although recorded by four or more stations, the microearthquake could not be precisely located using the recorded P arrival and estimated origin time.

The relative locations of Class B events are within ±5.0 km in geographic location. No attempt was made to calculate Class B depths of focus.

RESULTS

Location of Microearthquakes

1. Geographic Distribution

The epicenters for 58 Class A microearthquakes are plotted in Figure 11. Corresponding locations and origin times are listed in Table 2. In the Socorro area, multiple shocks and swarms of microearthquakes commonly take place at the same hypocenter over a short period of time (e.g. 6 hours). Thus one epicenter on Figure 11 may represent the location of many microearthquakes. The column entitled N in Table 2 (and Table 3) lists the number of shocks represented by each epicenter. Altogether, 298 separate microearthquakes occurred at the 58 epicenters plotted on Figure 11.

Similarly, the epicenters of 30 Class B microearthquakes are plotted on Figure 12 and their origin times and locations are listed in Table 3. Again, because of multiple events and swarms, the 30 epicenters are the locations for 61 separate microearthquakes.

On a regional basis the microearthquake epicenters indicate a band of seismic activity on the axis of the Rio Grande rift (Figures 11 and 12). The primary exception to this pattern is a narrow finger of activity which extends southeast from Socorro into an area near the rift's eastern margin. The regional pattern of epicenters observed in this study is in agreement with the findings of Sanford et al. (1972) (Figure 5). This suggests that the pattern described above

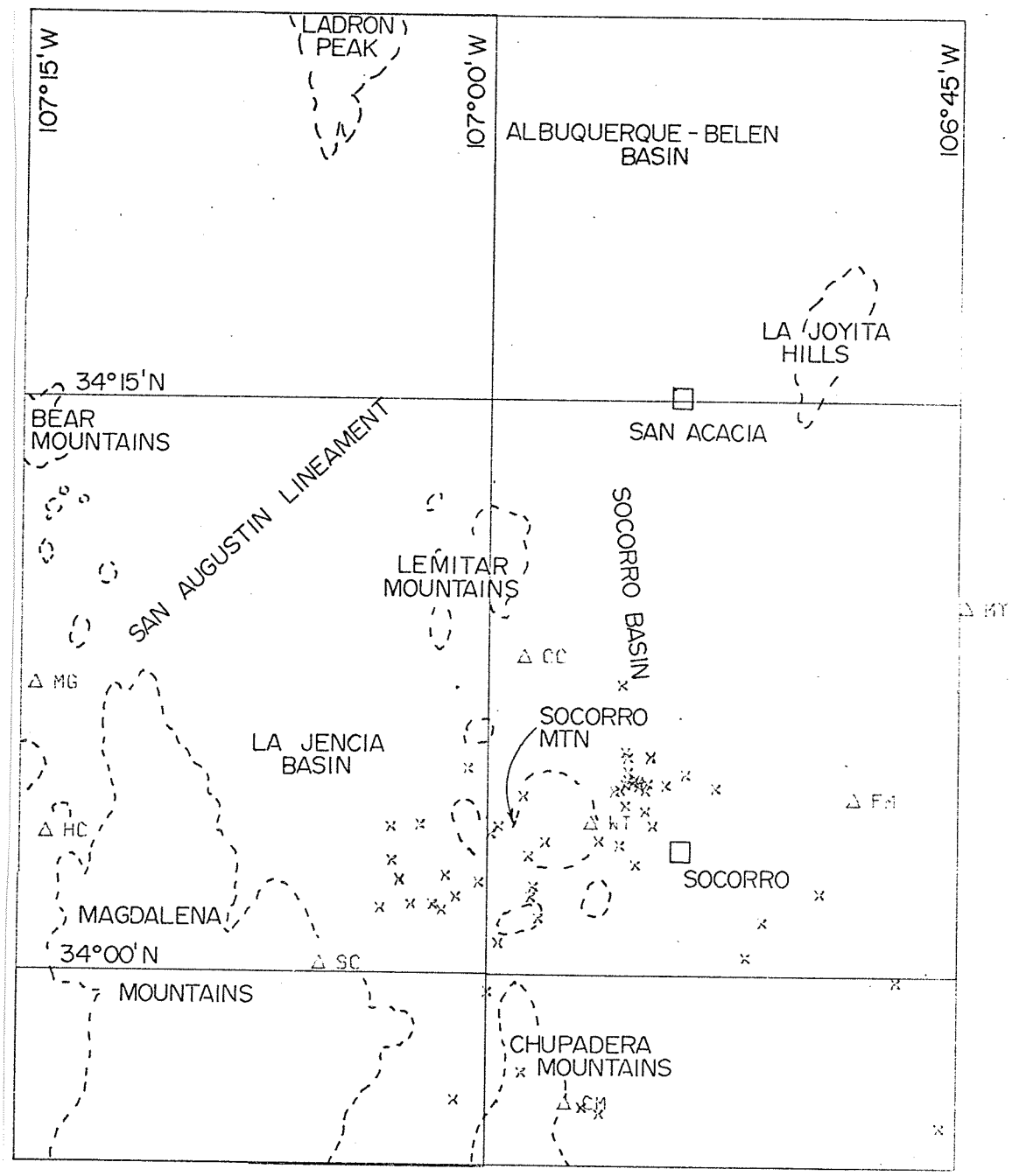

Figure 11. Map showing the Class A locations of epicenters for microearthquakes occurring near Socorro from April 15 through December 15, 1975. X's indicate epicenters; open triangles indicate seismic stations.

Table 2. Class A Microearthquake Locations

Date	Origin Time	Latitude	Longitude	Depth*	N**
May 20, 1975	04:25:09.20	33.9427	106.9488	4.97	2
May 20, 1975	17:10:01.60	34.0946	106.9144	9.35	2
May 22, 1975	10:27:08.50	34.0815	106.8794	3.95	1
May 22, 1975	11:36:29.03	33.9397	106.9395	4.75	1
May 26, 1975	23:45:51.30	34.0775	106.9810	7.99	1
May 29, 1975	07:14:12.12	33.9452	107.0168	9.58	1
Jun 3, 1975	02:45:09.60	34.0826	106.9062	3.34	12
Jun 3, 1975	04:48:17.80	34.0844	106.9204	9.29	1
Jun 3, 1975	15:10:15.60	34.0301	107.0296	10.34	1
Jun 16, 1975	23:43:21.11	34.0276	107.0242	10.80	1
Jun 17, 1975	15:30:45.14	34.0647	106.9129	7.35	1
Jun 17, 1975	18:50:33.31	34.0640	107.0520	10.60	2
Jun 26, 1975	02:56:45.11	34.0647	107.0365	6.11	2
Jul 1, 1975	13:35:58.50	34.0301	107.0408	9.96	1
Jul 9, 1975	02:12:24.80	34.0562	106.9302	6.11	6
Jul 9, 1975	09:16:47.97	34.0804	106.9167	8.67	2
Jul 23, 1975	14:56:41.62	34.0281	107.0576	13.00	3
Jul 24, 1975	04:23:14.30	34.0646	106.9940	5.18	1
Jul 30, 1975	21:44:42.10	34.0848	106.9223	8.23	1
Aug 5, 1975	02:26:02.50	34.0335	106.9772	7.58	8
Aug 5, 1975	04:17:20.92	34.0379	106.9758	7.78	1

* DATUM FOR DEPTH OF FOCUS CALCULATIONS - 1666 m.a.s.l.

** NUMBER OF EVENTS AT THE SAME HYPOCENTER

Table 2. Continued

Date	Origin Time	Latitude	Longitude	Depth*	N**
Aug 8, 1975	10:53:58.00	34.0837	106.9233	6.69	2
Aug 8, 1975	10:57:22.59	34.0796	106.9329	6.80	6
Aug 12, 1975	03:59:36.10	33.9574	106.9812	3.95	1
Aug 12, 1975	07:09:11.15	34.0357	106.8225	0.00	1
Aug 12, 1975	15:25:28.30	34.0513	106.9785	8.78	1
Aug 13, 1975	05:19:18.20	34.0823	106.9207	8.15	27
Aug 13, 1975	07:39:18.40	34.0826	106.9274	7.92	1
Aug 13, 1975	11:22:26.90	34.0245	106.9731	9.05	1
Aug 13, 1975	20:18:25.62	34.0894	107.0109	8.50	1
Aug 15, 1975	06:36:45.80	34.0871	106.8957	7.28	2
Aug 19, 1975	08:11:46.60	34.0580	106.9409	10.93	2
Aug 19, 1975	10:00:07.20	33.9922	107.0000	10.88	1
Aug 19, 1975	20:10:22.60	34.0971	106.9276	9.16	4
Aug 20, 1975	05:22:19.70	34.0882	106.9261	10.05	15
Aug 20, 1975	12:20:52.35	34.0833	106.9153	7.01	2
Aug 20, 1975	15:29:36.60	34.0848	106.9261	6.94	2
Aug 20, 1975	21:59:44.30	34.0947	106.9261	8.91	6
Aug 21, 1975	03:44:48.70	34.0407	107.0470	9.51	1
Aug 21, 1975	19:04:06.50	34.0575	106.9692	7.54	10
Aug 25, 1975	19:37:41.10	34.0714	106.9167	6.73	5
Aug 26, 1975	08:40:15.40	34.0480	106.9220	9.40	12
Aug 28, 1975	01:26:02.50	34.1264	106.9296	2.87	5
Aug 29, 1975	08:52:18.80	34.0737	106.9271	7.19	20

Table 2. Continued

Date	Origin Time	Latitude	Longitude	Depth*	N**
Sep 16, 1975	13:30:52.55	34.0804	106.9301	6.66	1
Sep 19, 1975	08:42:57.21	34.0234	106.8539	5.52	1
Sep 24, 1975	02:17:09.30	34.0954	106.9140	7.25	7
Oct 29, 1975	07:21:35.35	34.0609	106.9987	3.87	4
Oct 29, 1975	20:50:49.60	34.0134	106.9940	4.76	2
Oct 30, 1975	07:09:39.20	34.0335	107.0168	5.59	1
Oct 31, 1975	04:02:15.27	33.9345	106.7589	9.59	1
Nov 4, 1975	16:30:12.10	34.0491	107.0517	6.24	31
Nov 5, 1975	02:40:10.50	33.9973	106.7823	9.83	1
Nov 5, 1975	14:35:05.50	34.0402	107.0475	7.60	22
Nov 5, 1975	22:28:26.70	34.0424	107.0228	4.45	19
Nov 6, 1975	09:33:59.20	34.0396	107.0047	7.98	2
Nov 6, 1975	11:05:48.30	34.0078	106.8629	7.97	1
Nov 7, 1975	08:27:36.10	34.0480	107.0323	7.09	25

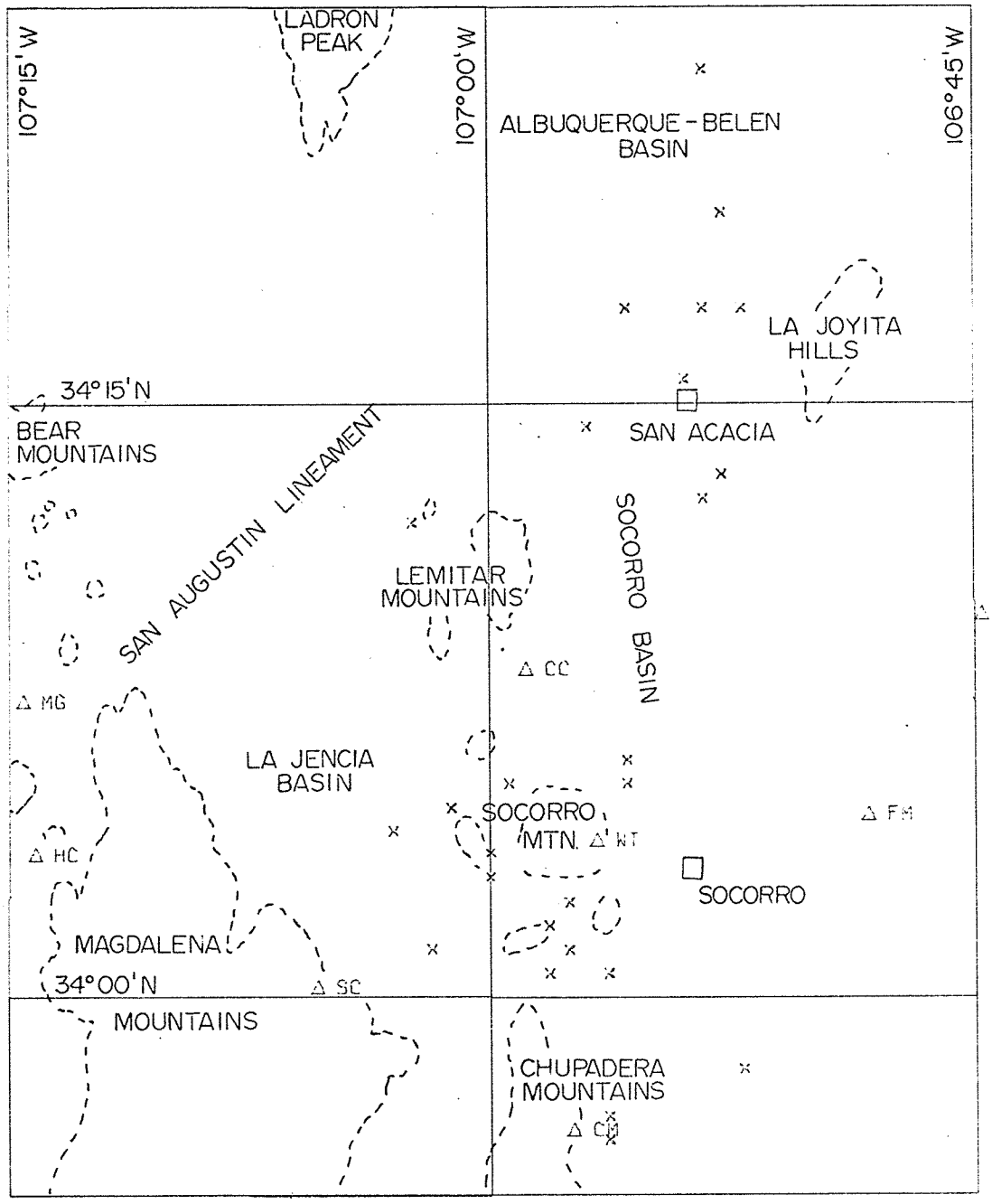

Figure 12. Map showing the Class B locations of epicenters for microearthquakes occurring near Socorro from April 15 to December 15, 1975. X's indicate epicenters.

Table 3. Class B Microearthquake Locations

Date	Origin Time	Latitude	Longitude	N*
Apl 17, 1975	00:02:18.40	34.2200	106.8800	4
Apl 17, 1975	17:31:07.70	33.9700	106.8700	2
May 20, 1975	10:34:23.30	33.9400	106.9400	1
May 20, 1975	13:20:40.00	34.2900	106.9300	1
May 22, 1975	13:19:41.40	33.9500	106.9400	1
Jun 3, 1975	04:03:00.70	34.0900	106.9900	1
Jun 4, 1975	04:20:14.20	34.0100	106.9400	1
Jun 17, 1975	00:00:54.10	34.0800	107.0200	1
Jun 17, 1975	02:19:53.90	33.9400	106.9400	1
Jun 24, 1975	20:47:34.50	34.3300	106.8800	1
Jul 2, 1975	01:00:19.25	34.2200	106.8800	2
Jul 3, 1975	16:12:20.90	34.0100	106.9700	1
Jul 9, 1975	07:55:42.20	34.2600	106.9000	1
Jul 22, 1975	00:29:19.20	34.2400	106.9500	1
Jul 22, 1975	00:45:34.50	34.0400	106.9600	3
Jul 24, 1975	17:10:14.25	34.0200	107.0300	1
Jul 24, 1975	18:50:19.20	34.2900	106.8700	1
Aug 1, 1975	11:26:20.90	34.0800	107.0200	1
Aug 5, 1975	14:19:22.13	34.0700	107.0500	2
Aug 6, 1975	20:12:33.20	34.0300	106.9700	1
Aug 13, 1975	05:29:49.48	34.2000	107.0400	1
Aug 14, 1975	05:16:15.10	34.2900	106.8900	1
Aug 14, 1975	19:03:28.30	34.1000	106.9300	5

* NUMBER OF EVENTS AT SAME EPICENTER

Table 3. Continued

Date	Origin Time	Latitude	Longitude	N*
Aug 15, 1975	07:33:52.40	34.0200	106.9600	2
Aug 19, 1975	02:14:21.60	34.2100	106.8900	1
Aug 22, 1975	00:35:05.60	34.0300	106.9700	1
Aug 27, 1975	07:35:13.20	34.0900	106.9300	8
Sep 24, 1975	10:54:17.00	34.3900	106.8900	12
Oct 29, 1975	09:34:37.10	34.0500	107.0000	1
Oct 29, 1975	09:18:23.60	34.0600	107.0000	1

is representative of the microearthquake distribution for the past 10 years.

The major structural features which have microearthquake activity (Figures 11 and 12) are 1) the area near or within Socorro basin centered approximately 5 km north-northwest of Socorro, 2) the graben or possible caldera between the Socorro and Chupadera Mountains, 3) the northern end of the Chupadera Mountains, 4) the southwestern margin of Socorro Mountain, and 5) the southern end of La Jencia basin. Although not associated with a major structural feature, the area between the Socorro and Albuquerque-Belen basins also has microearthquake activity. The major structural features which do not have microearthquake activity (Figures 11 and 12) are 1) La Joyita Hills, 2) the Socorro basin from 9 km north of Socorro to 5 km south of San Acacia, 3) the Magdalena Mountains, and 4) the San Augustin lineament. The Bear and Ladron Mountains also appear to lack seismic activity but may have been outside the detection range of the seismic arrays used in this study.

2. Depths of Focus

The frequency of occurrence versus depth of focus for the 298 Class A microearthquakes is plotted on the histogram in Figure 13. All depth of focus calculations made in this study were with respect to a datum which is an average of the elevations for the most frequently occupied stations, 1666 meters. The histogram shows that focal depths in the Socorro area range from 0.0-14.0 km, and that two-thirds of all the

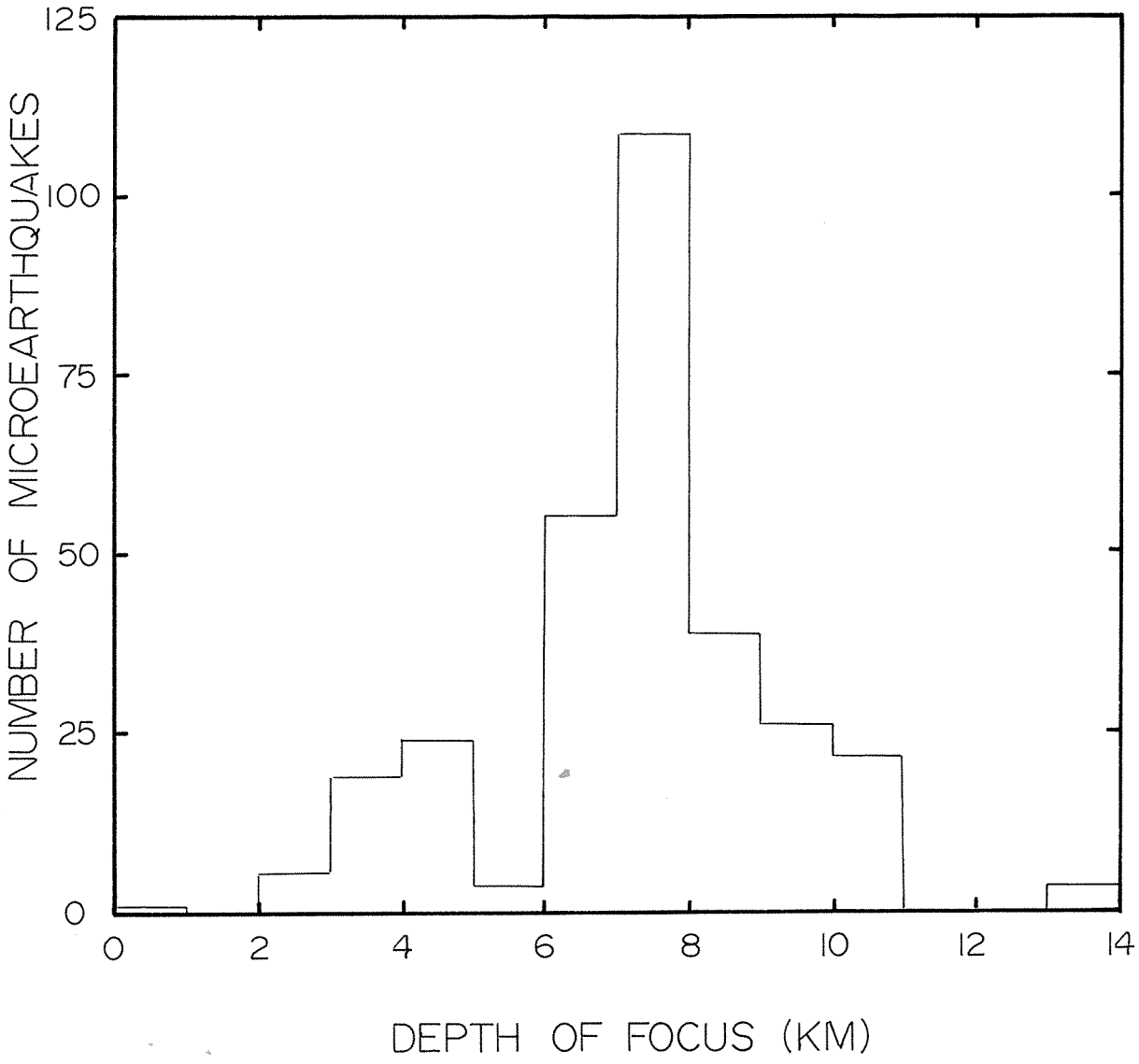

Figure 13. Histogram showing the number of microearthquakes versus the depth of focus for 298 Class A microearthquakes.

foci lie within a narrow band from 6.0 to 9.0 km beneath the surface.

The epicenters for microearthquakes occuring in the depth intervals 0.0-4.0 km, 4.0-8.0 km, and 8.0-12.0 km are plotted in Figures 14, 15, and 16, respectively. From these figures, all the seismically active structures appear to have foci which are scattered over a wide range of depths. The horizontal distribution of focal depths does not reveal any pattern which can be interpreted as a descending fault plane. In general, the depths of foci do not appear to have a significant geographic distribution.

The Relationship of Microearthquake Activity to Structural Geology

1. Faulting

The pattern of epicenters found in this study may in general be described as diffuse. Epicenters do not seem to form linear segments as might be expected to occur if activity was along single major faults. The locations of epicenters appear to be unrelated to major boundary faults separating basins from structural highlands. Similarly seismic activity within basins and highlands cannot, in general, be associated with known faults of any size. It should be noted that the epicenters 5 km north-northwest of Socorro lie along a north-trending normal fault. The fault offsets a Late Quaternary erosional surface within the Rio Grande valley and is downthrown on the western side. Although extending for several

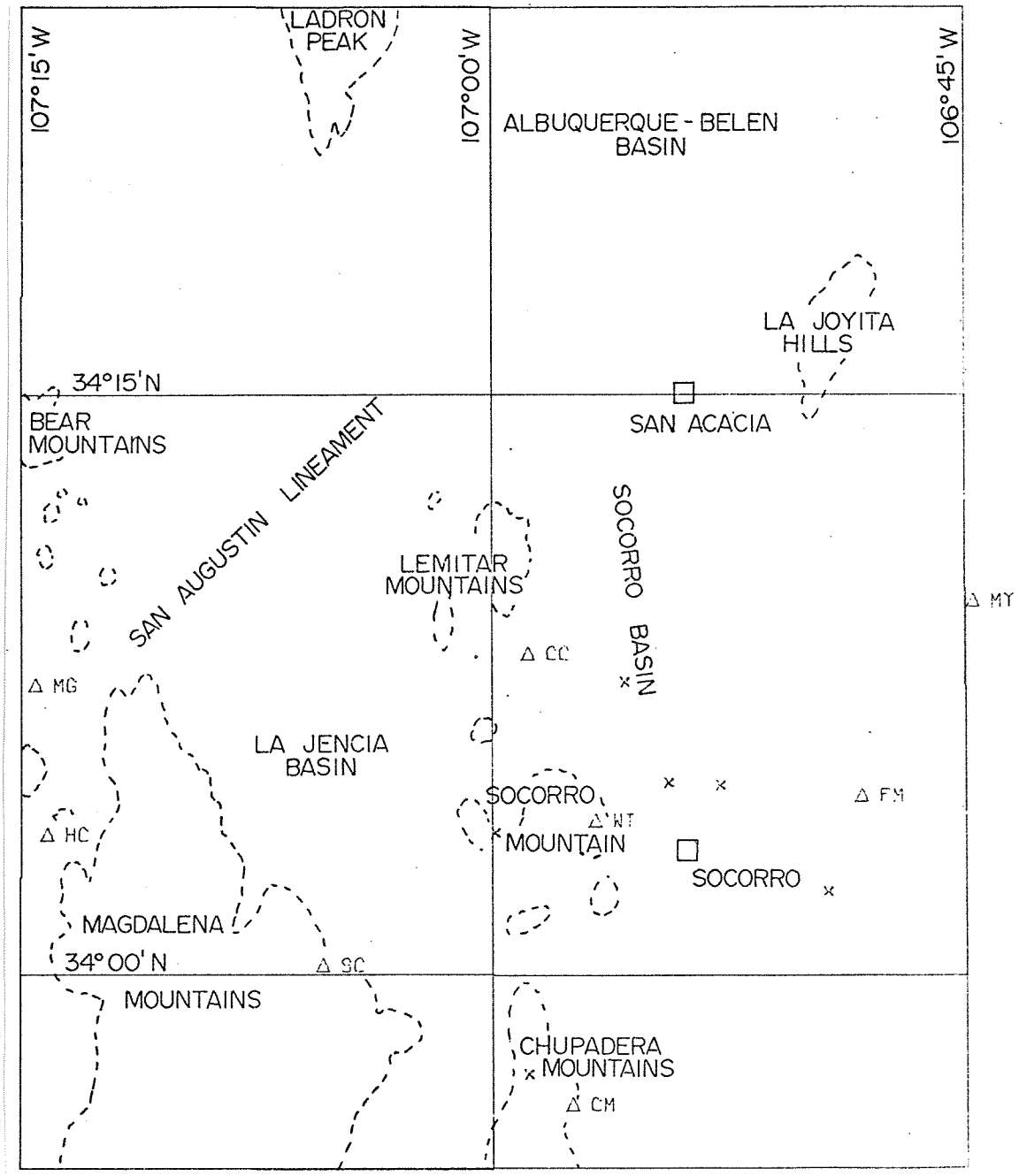

Figure 14. Map of Class A locations for microearthquakes with focal depths from 0.0 to 4.0 km. X's indicate epicenters.

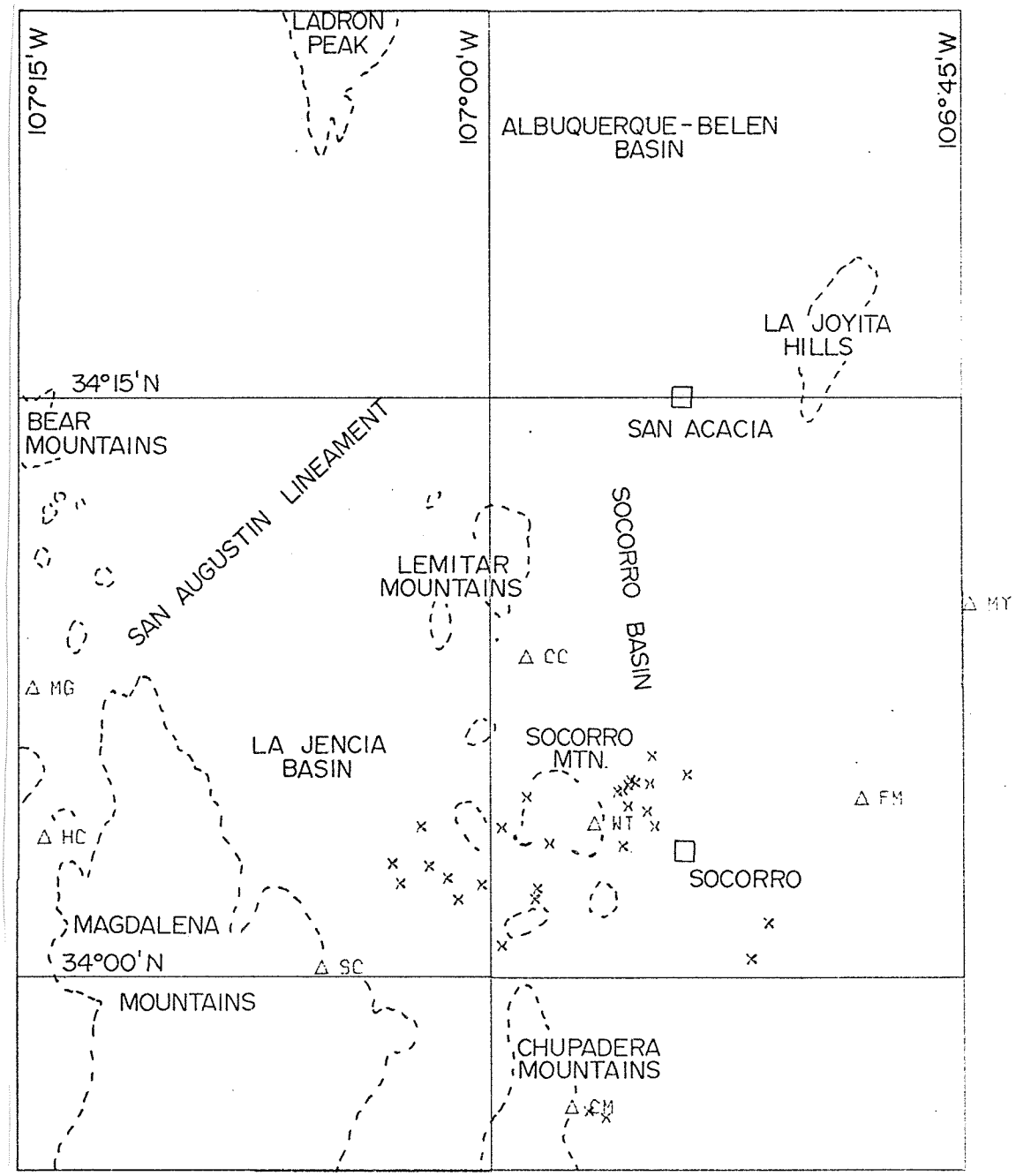

Figure 15. Map of Class A locations for microearthquakes with focal depths from 4.0 to 8.0 km. X's indicate epicenters.

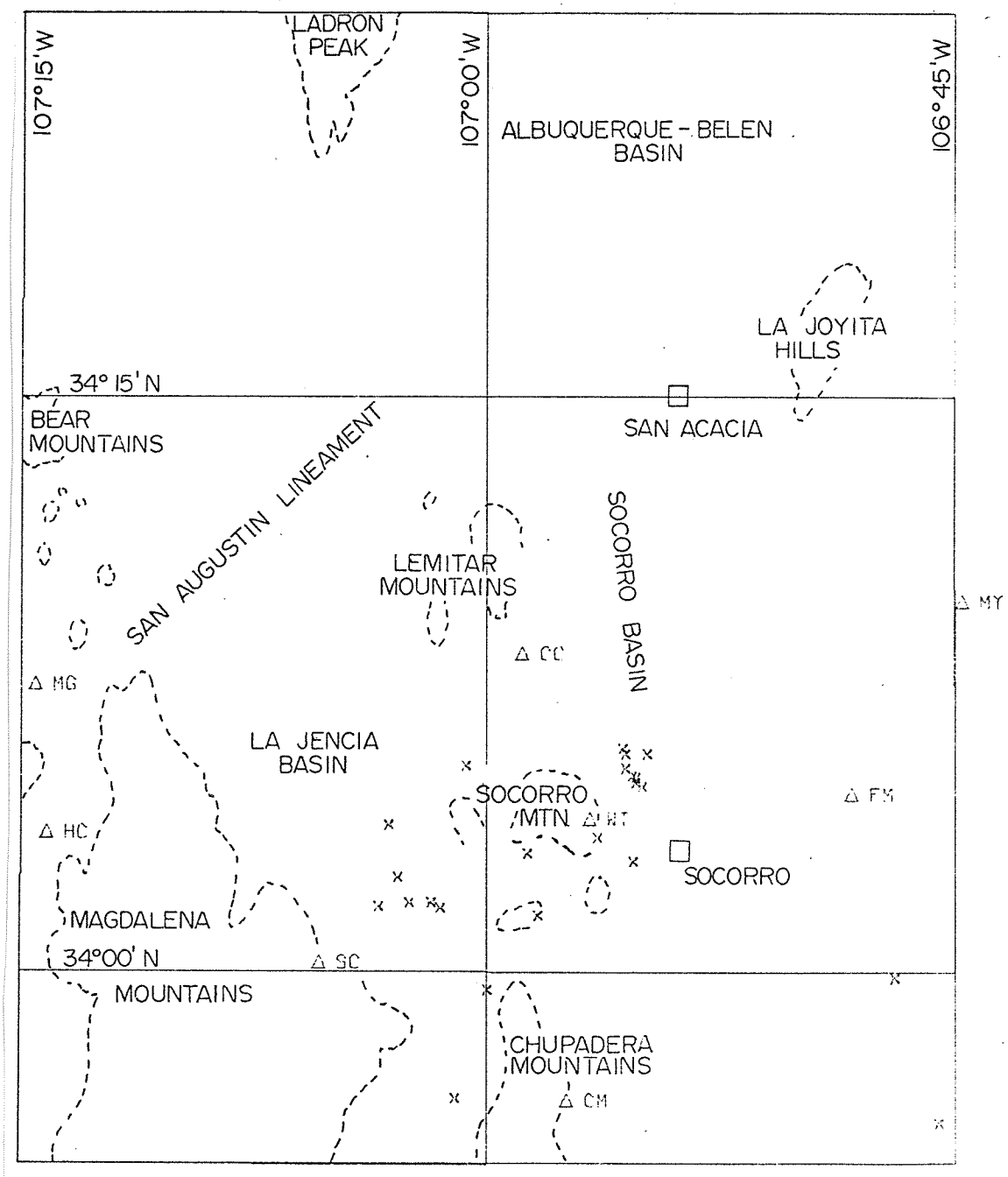

Figure 16. Map of Class A locations for microearthquakes with focal depths from 8.0 to 12.0 km. X's indicate epicenters.

kilometers and having more than three meters of displacement, this particular fault has only recently been fully mapped by Chamberlin (personal communication). Thus the apparent lack of correlation between the distribution of epicenters and known faults may be proven incorrect with more detailed geologic mapping in the area.

2. Fault-Plane Solutions

Figure 17 shows three composite fault-plane solutions constructed for microearthquakes in the Socorro region. Fault-plane solution A represents 16 microearthquakes with an average focal depth of 7.9 km in the area (discussed in the previous paragraph) 5 km north-northwest of Socorro. The solution indicates normal faulting on a plane striking north-northeast which is in agreement with the fault observed in the field. The fault-plane is chosen as dipping 40° to the west because the mapped fault is downthrown on the western side. Fault-plane solution B represents six microearthquakes with an average focal depth of 8.2 km in the graben or caldera between the Socorro and Chupadera Mountains. The solution indicates normal faulting on a plane striking north or north-northeast and dipping either 31°W or 60°E. Fault-plane solution C represents eight microearthquakes with an average depth of focus of 8.4 km in the southern end of La Jencia basin. The solution indicates either a composite of normal and right-hand strike-slip faulting on a plane striking N25°W and dipping 36°SW, or a composite of normal and left-

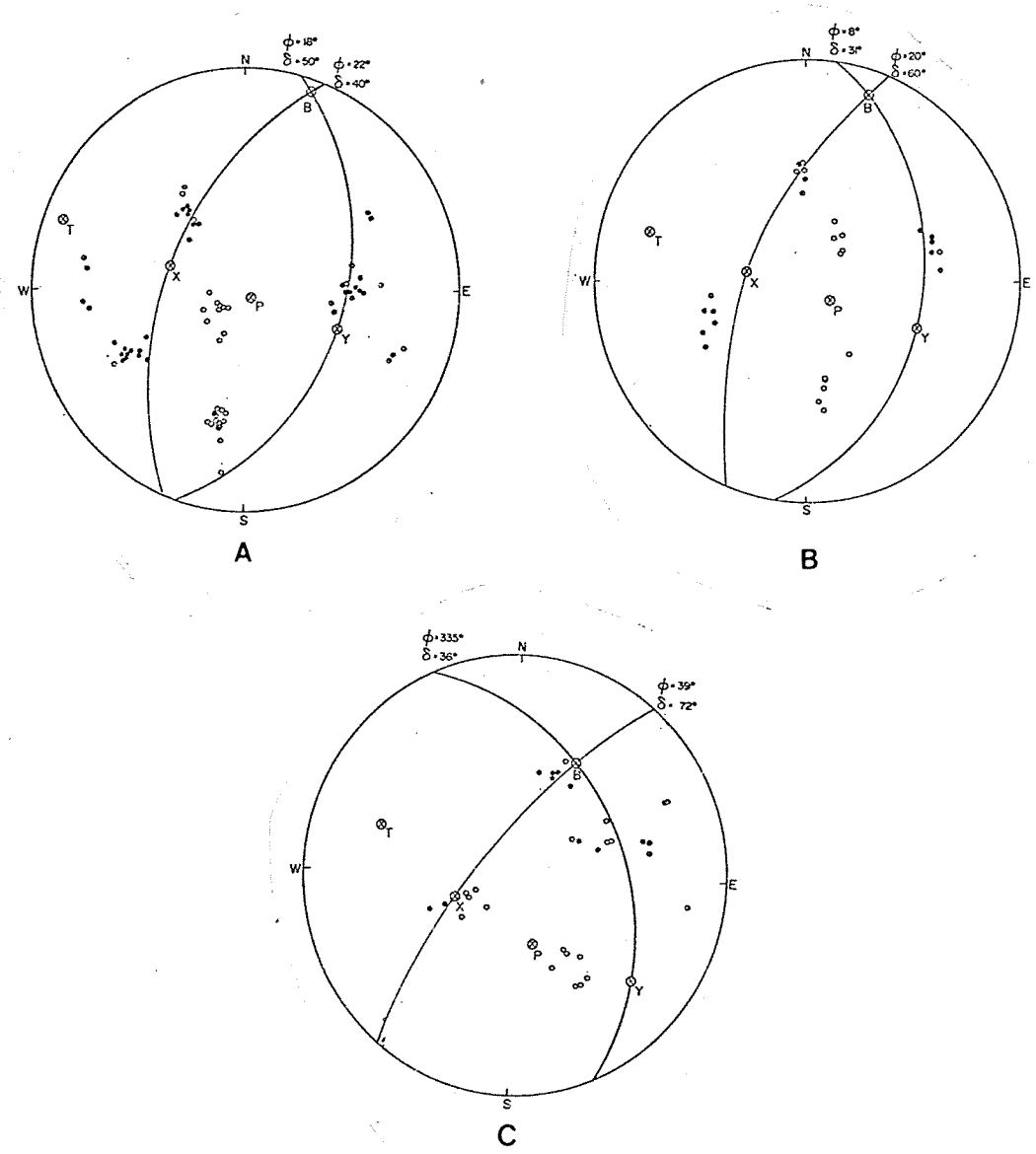

Figure 17. Three composite fault-plane solutions constructed from Class A microearthquakes. Solutions A, B, and C represent shocks in the area 5 km north-northwest of Socorro, in the graben between the Socorro and Chupadera Mountains, and in the southern end of La Jencia basin, respectively. Open circles indicate dilatations; solid circles indicate compressions.

hand strike-slip faulting on a plane striking N39°E and dipping 72°SE.

In Figure 18, the epicenters for 39 shocks are plotted with symbols which indicate the type of initial P motion (compressive or dilatational) at seismic station WT. The first motions for 82% of the events shown in Figure 18 are dilatations. For areas where strike slip is prevalent, a quadrantal pattern of compressions and dilatations centered on the seismic station is expected. The pattern observed in the Socorro area is far from quadrantal, and thus significant strike-slip faulting cannot be occurring. The fact that dilatations occur nearly everywhere in the vicinity of Socorro indicates that the dominant type of dipslip movement is normal.

In Figure 17 the P axes, representing the axes of greatest principal stress, have orientations S40°E, S52°E, and S18°E with corresponding plunges of 85°NW, 75°NW, and 54°NW. Similarly the T axes, representing the axes of least principal stress, have the orientations N70°W, N73°W, and N72°W with corresponding plunges of 5°SE, 15°SE, and 22°SE. A west-northwest-trending least principal (tensional) stress agrees well with the east-west tensional tectonic regime frequently described in literature for the Rio Grande rift.

Chapin and Seager (1975) have suggested a thin-skinned distensional faulting process for the formation in Late Miocene-Pliocene time of the Socorro-Lemitar Mountains. This process was first described by Anderson (1971) for an

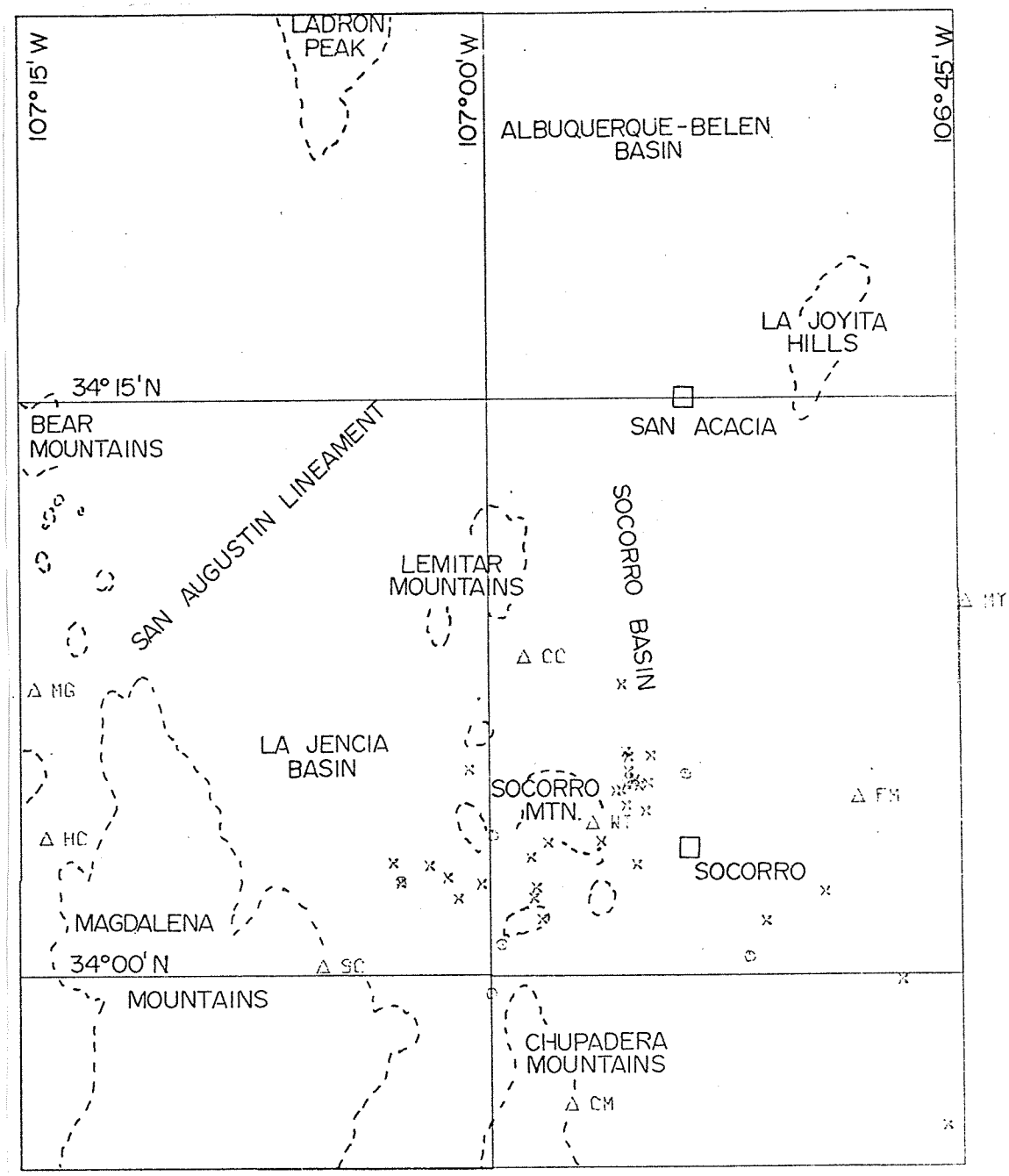

Figure 18. Map of Class A epicenters with symbols indicating the type of initial P motion received at seismic station WT. X's indicate dilatations; open circles indicate compressions.

area in southeastern Nevada. It requires high-angle normal faults to bend into horizontal faults at shallow depths (i.e. 0.5-2.0 km beneath the surface). The normal faulting, which parallels the margins of the Socorro-Lemitar Mountains, is in agreement with the proposed thin-skinned distension model. A major disagreement between seismological data and the thin-skinned distension model is the depth at which the majority of faulting must occur. Anderson's model produces the majority of faulting within the interval from 0.0 to 2.0 km. Microearthquakes near Socorro indicate that currently less than 1% of the faulting is taking place in this interval (while 65% of the faulting occurs between 6.0-9.0 km.) This result indicates either the Anderson thin-skinned distension model is not fully applicable to the Socorro region, or the process of thin-skinned distension has terminated and currently some other type of faulting process is taking place.

3. Volcanism and Magmatism

Earthquake swarms, that is a long series of small and large shocks with no one outstanding principal event, are common in volcanic regions and regions of geologically recent but not current volcanism (Richter, 1958). Swarms beneath Hawaii are associated with the collection of magma into conducting channels at depth and the movement of magma towards the surface (Eaton and Murata, 1960). Swarms beneath the oceans generally occur at spreading centers along mid-oceanic ridges (Sykes, 1970). The inflation of a magma chamber at

shallow depth has been suggested as the triggering mechanism for the Matsushiro, Japan earthquake swarm of 1965-1967 (Stuart and Johnston, 1975). Earthquake swarms have also been associated with some geothermal areas of the world although they are notably absent from others.

In the Socorro region, recent and current magmatic processes are indicated from both geological and geophysical evidence. Volcanism has taken place near Socorro intermittently since Oligocene time. The most recent volcanism, andesitic basalt flows, occurred during the Late Tertiary or Quaternay in the structural low between the Socorro and Chupadera Mountains and in the Rio Grande valley near San Acacia. In general the entire western section of the Rio Grande Rift is a major geothermal anomaly with a heat flow value of greater than 2.5 HFU (Reiter et al., 1975). The heat flow within Socorro Mountain is exceptionally high with a value of 11.5 HFU (Sanford and Reiter, manuscript in preparation). The most conclusive evidence for current magmatism is a magma layer at 18 km beneath Socorro which has been mapped using reflected phases from microearthquakes (Sanford et al., 1973).

Historically, major earthquake swarms occurred near Socorro in 1904 and 1906-1907 (Sanford, 1963). The swarm of 1904 commenced on January 19 and terminated in September. At least 34 shocks were felt with intensities ranging up to VII. The second swarm began July 2, 1906 and ended sometime in the early part of 1907. Shocks were felt almost daily and during this swarm three events reached intensity VIII. On

the basis of intensity data and other evidence, Sanford (1963) determined the epicenters for both swarms were close to Socorro and most likely beneath the Socorro Mountain block.

Seventeen microearthquake swarms with Class A locations are plotted on Figure 19. A swarm in this discussion is defined as five or more microearthquakes with the same hypocenter occurring over an interval of 6 hours or less. The geographic pattern for swarms are confined to 1) the area north-northwest of Socorro, 2) the graben or caldera between the Socorro and Chupadera Mountains, and 3) the southern end of La Jencia basin.

The frequency of occurrence versus depth of focus for the 17 swarms is graphed in Figure 20. The distribution of swarms foci is very similar to that of all microearthquakes (Figure 13). The focal depths of 76% of the swarms occur between 6.0 and 9.0 km.

In the region studied in this report, numerous major structural features have been created by large-scale faulting but locations of recent volcanism are confined to the areas near Socorro Mountain and San Acacia. San Acacia is seismically active and the known location of swarms (Sanford et al., 1972). Microearthquake swarms are associated with the area around Socorro Mountain both currently and historically. Specific swarms cannot be associated with volcanic flows observed at the surface. Most notably the 11 swarms north-northwest of Socorro are located within the Rio Grande valley in an area which appears to be unaffected by the most recent

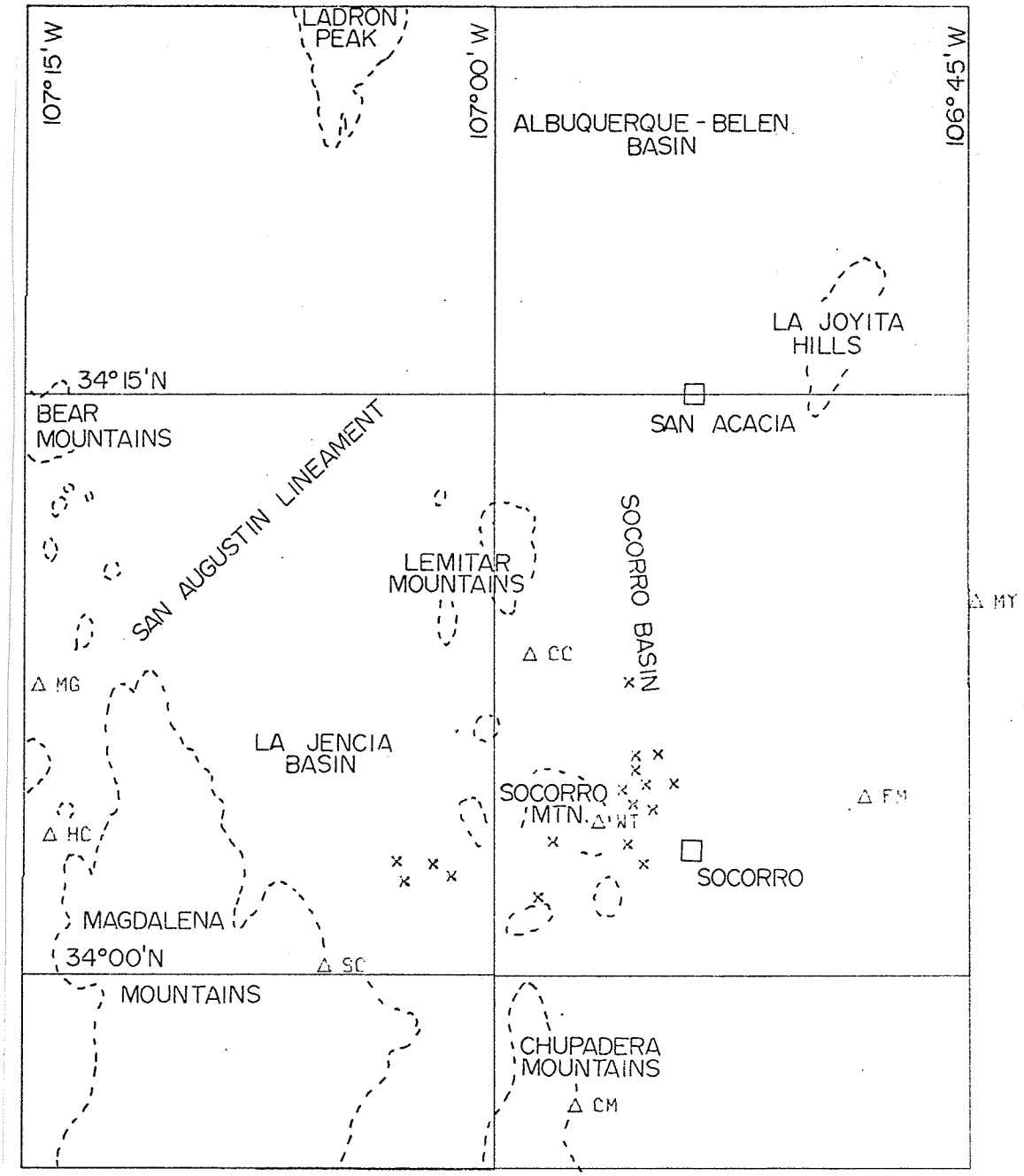

Figure 19. Map of Class A locations of epicenters for micro-earthquake swarms occurring near Socorro from April 15 to December 15, 1975. X's indicate epicenters.

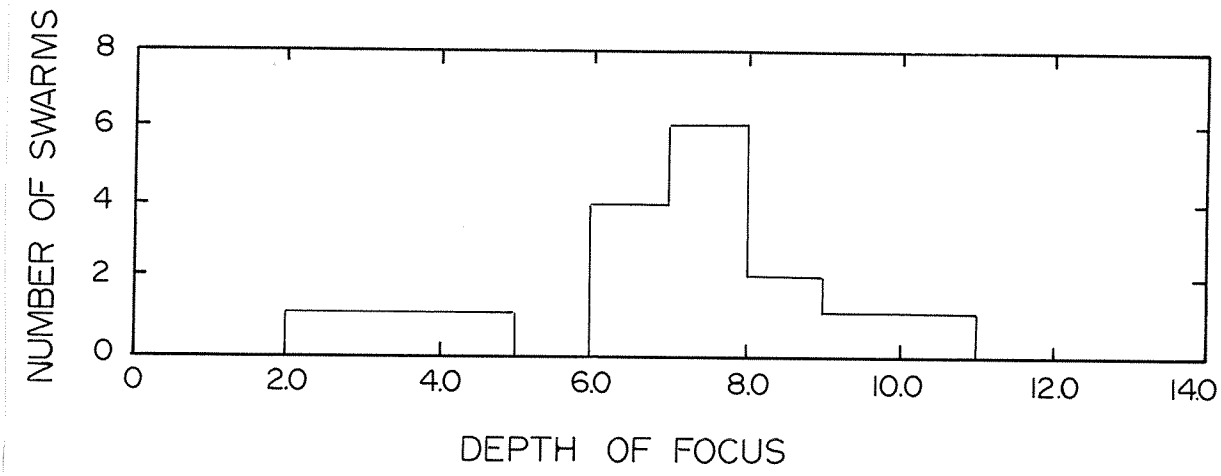

Figure 20. Histogram showing the number of microearthquake swarms versus depth of focus for the Socorro region.

episodes of volcanism. Instead, the 11 swarms are located along the normal fault discussed in the previous section. Thus although there appears to be a general association between the volcanic activity and microearthquake swarms observed near Socorro Mountain, it cannot be extended to associate the swarms to known volcanic centers or magmatic processes. Four possible explanations for this observation are: 1) the inflation of a magma chamber is acting as a triggering mechanism for pre-existing faults; 2) magma is moving along major faults and is again operating as a triggering mechanism; 3) magma is moving along conduits which have never breached the surface; and 4) magma is stoping its way to the surface and therefore generating a new conduit. For the Socorro Mountain area, it is also possible a direct association between current or recent volcanism and microearthquake swarms does not exist and thus the swarms are being generated by some other unknown process.

A Magma Layer Mapped By Reflected Phases From Microearthquakes

A magma layer at 18 km depth beneath Socorro was mapped by Sanford and Long (1965) and Sanford et al. (1973) using reflected S_XS and S_XP phases generated by microearthquakes. Following the same procedure but using only S_XS phases, the depths and locations of 90 reflections off the same layer have been found in this study. The points of reflection on the surface of the magma layer are plotted in Figure 21. The X's are reflection points calculated from phases on Class A

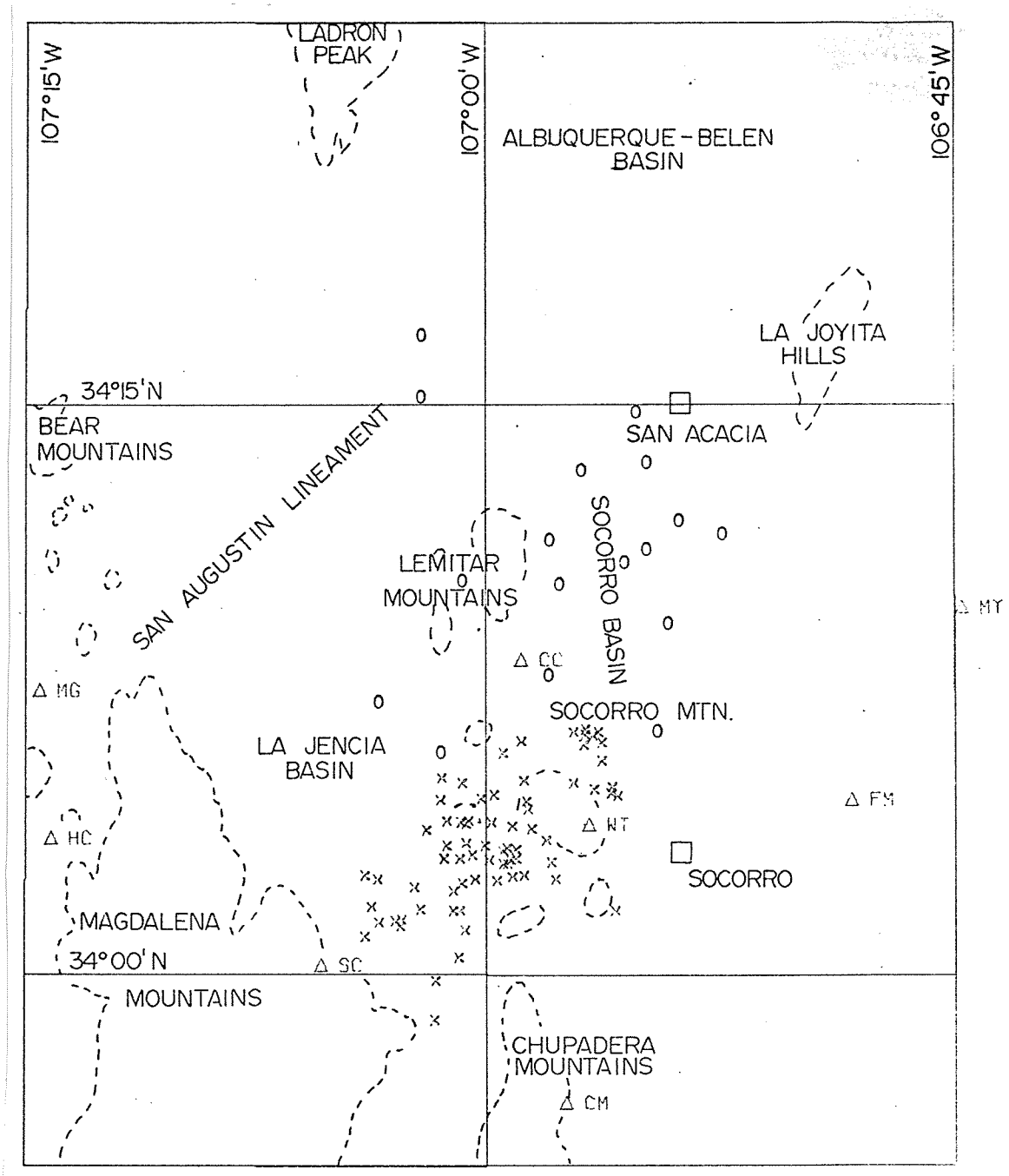

Figure 21. Map of points of reflection on the surface of the magma layer for S_xS microearthquake phases. X's indicate good reflection points calculated from Class A microearthquake locations. Open circles indicate reflection points estimated from Class B microearthquake locations.

microearthquakes which are accurately located. The 0's are reflection points estimated from reflection phases on Class B events and are quite inaccurate because focal depths were assumed to be 7 km.

The map of reflection points (Figure 21) indicates the magma layer occupies a minimum area of approximately 500 km^2. Sanford et al. (1973) found the magma layer to be approximately 11 km wide and to exist along a north-northeast axis from 5 km southwest of Socorro to 50 km northeast. The points of reflection found in this study widen the magma layer to approximately 15 km, extend the layer to a position 8.5 km southwest of Socorro, and indicate an overall more northerly trend.

The limits for the magma layer are generally unknown although there is some indication the layer may terminate or at least become discontinuous to the southeast beginning beneath the city of Socorro. Evidence in favor of the interruption of the magma layer in this area is twofold. First, stations FM and CM have recorded a disproportionately small number of reflections (6% and 11% of the total reflection for the five most frequently occupied stations). Fault plane solutions indicate that the lack of reflections cannot be fully explained by the radiation pattern of S-phase energy from the earthquake foci. Second, five microearthquakes which have occurred from 4 to 15 km southeast of Socorro did not produce reflections at any seismic station. Both of the above observations are most easily explained by the absence of the magma layer.

Figure 22 is a histogram showing the number of reflections (Class A data) versus the calculated depth to the magma surface. Values for the depth range from 16.0 to 24.0 km and average 20.0 km. Errors in calculated depths arise primarily from the inaccuracies in hypocenter locations and errors in identifying and timing the onset of S_XS phases. Another factor affecting depth calculations may be lateral inhomogeneities in the crust. Figures 23 through 26 are maps of the reflection points occurring at progressively deeper intervals. From these it appears that the magma layer is shallowest, 17.0-19.0 km, just west and southwest of WT and deepens to greater than 21.0 km beneath the southern end of La Jencia basin. Further evaluation of the areal change in the depth to the magma layer is difficult because of scatter in the depths calculated.

A goal of the ongoing research has been to establish boundaries for the magma layer. To date, the limits to the magma layer have not been established but several observations can be made about the distribution of microearthquake activity relative to the known position of the magma layer. The area above the magma layer does not appear to be seismically active everywhere (eg. the Lemitar Mountains appear to be aseismic). If a boundary for the magma layer is assumed to occur beneath Socorro, seismic activity occurs well outside the area underlain by magma. Therefore microearthquake activity does not appear to be directly related to the presence or absence of the magma layer.

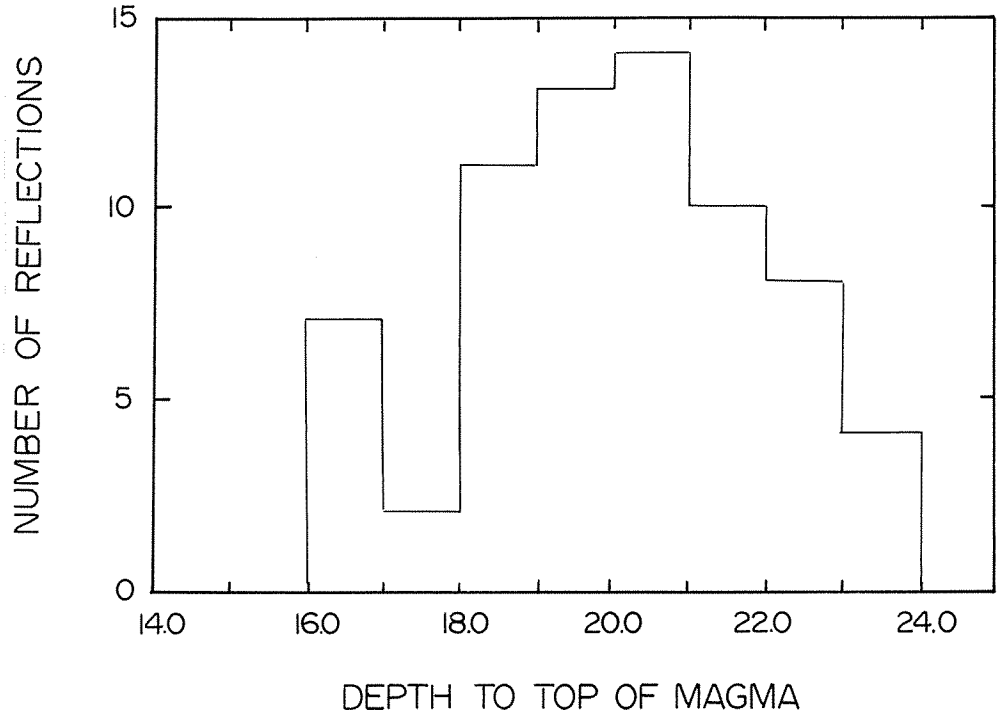

Figure 22. Histogram showing the number of reflections (from Class A data) versus depth calculated to the magma surface.

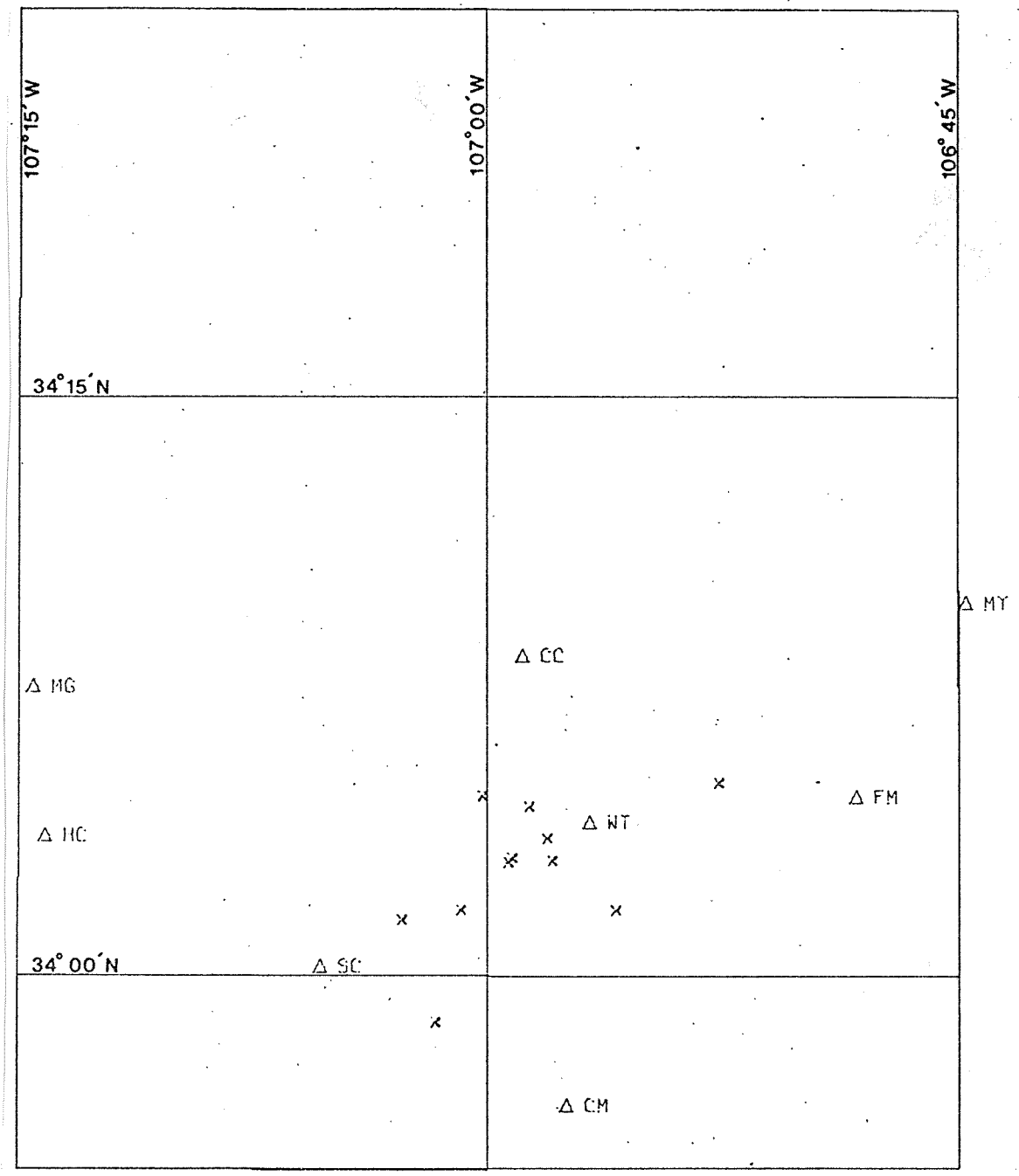

Figure 23. Map showing the S_XS points of reflection which indicate the magma layer occurs at less than 17.0 km depth.

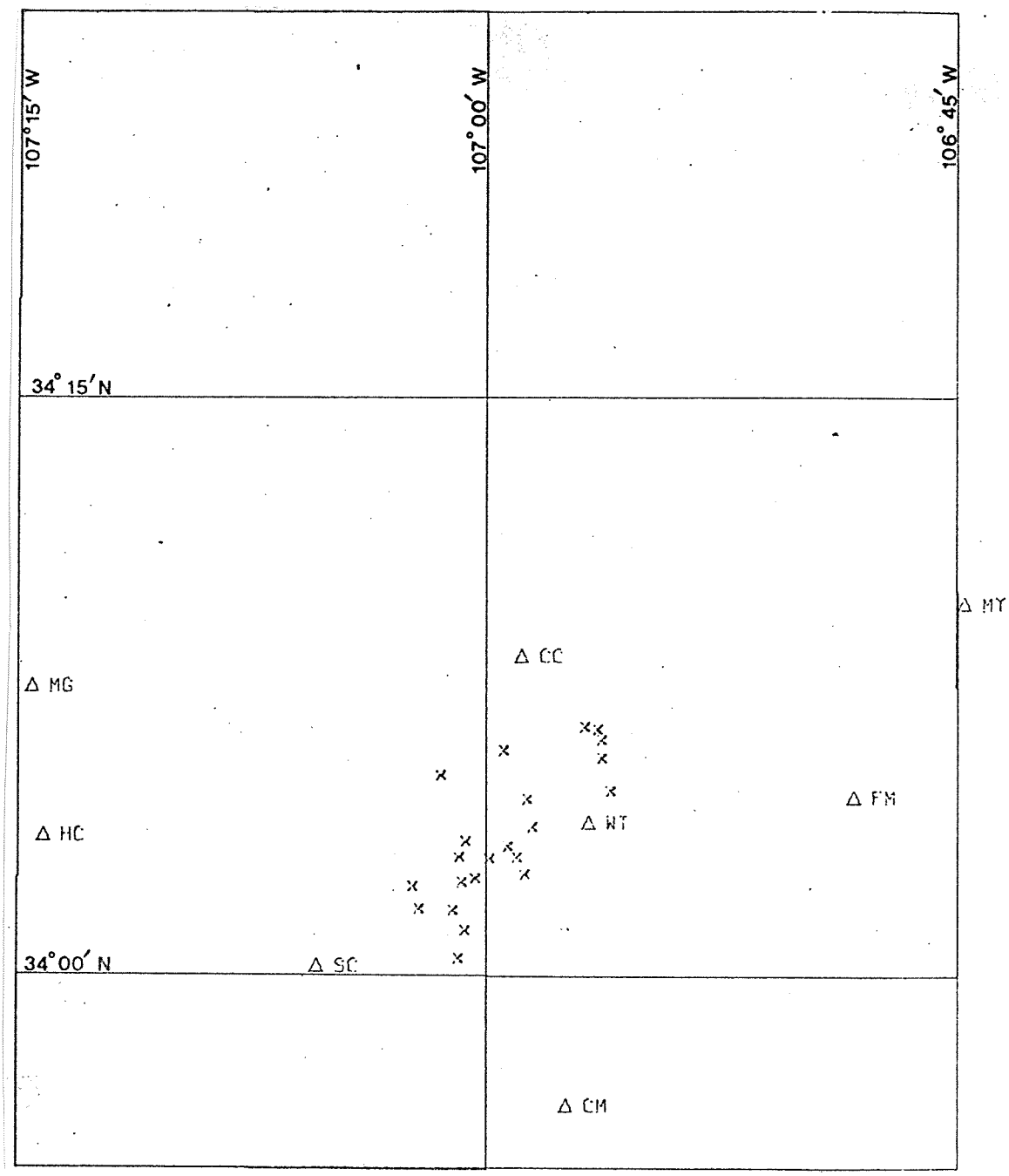

Figure 24. Map showing the S_XS points of reflection which indicate the magma layer occurs at a depth between 17.0 km and 19.0 km.

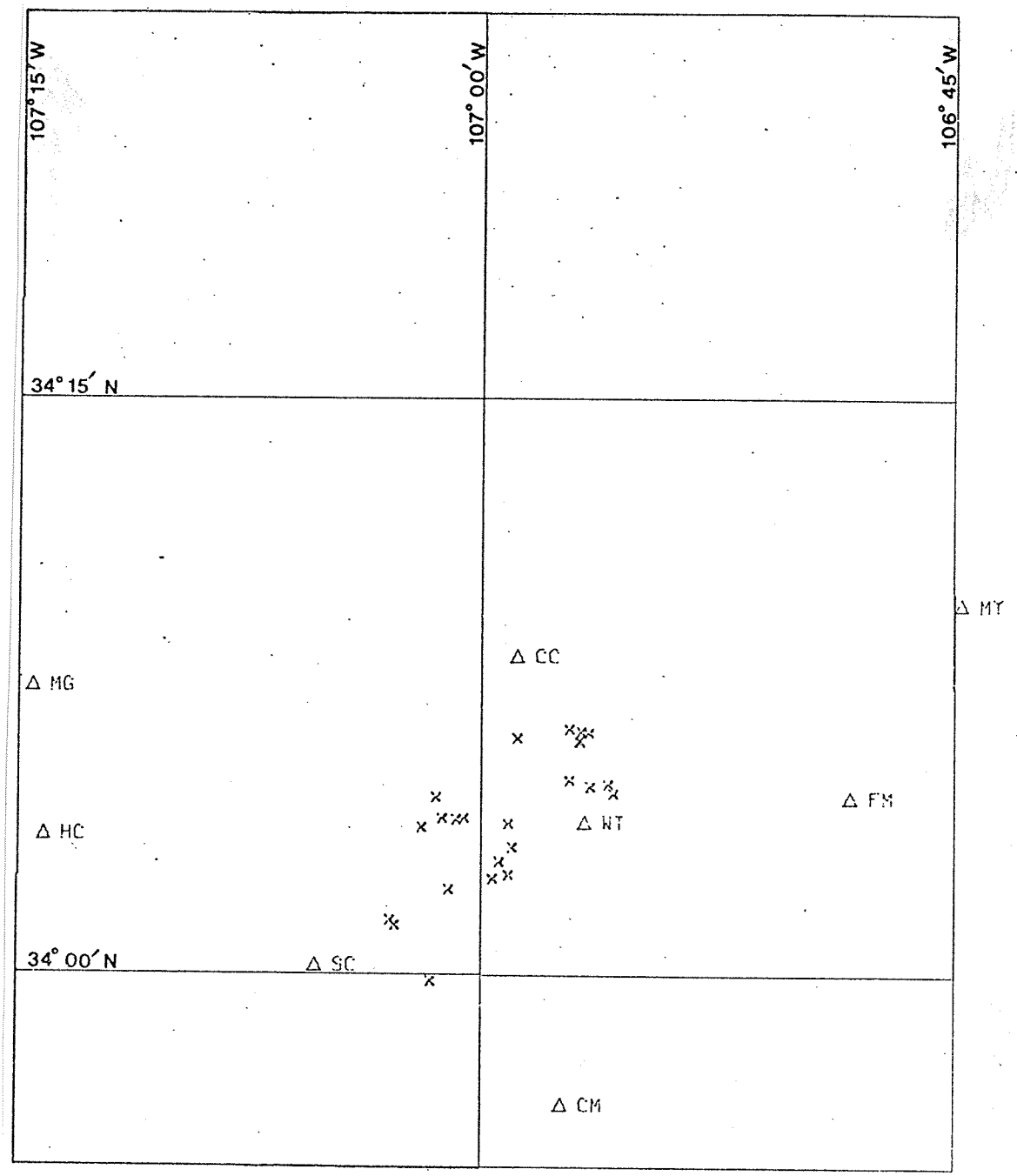

Figure 25. Map showing the S_XS points of reflection which indicate the magma layer occurs at a depth between 19.0 and 21.0 km.

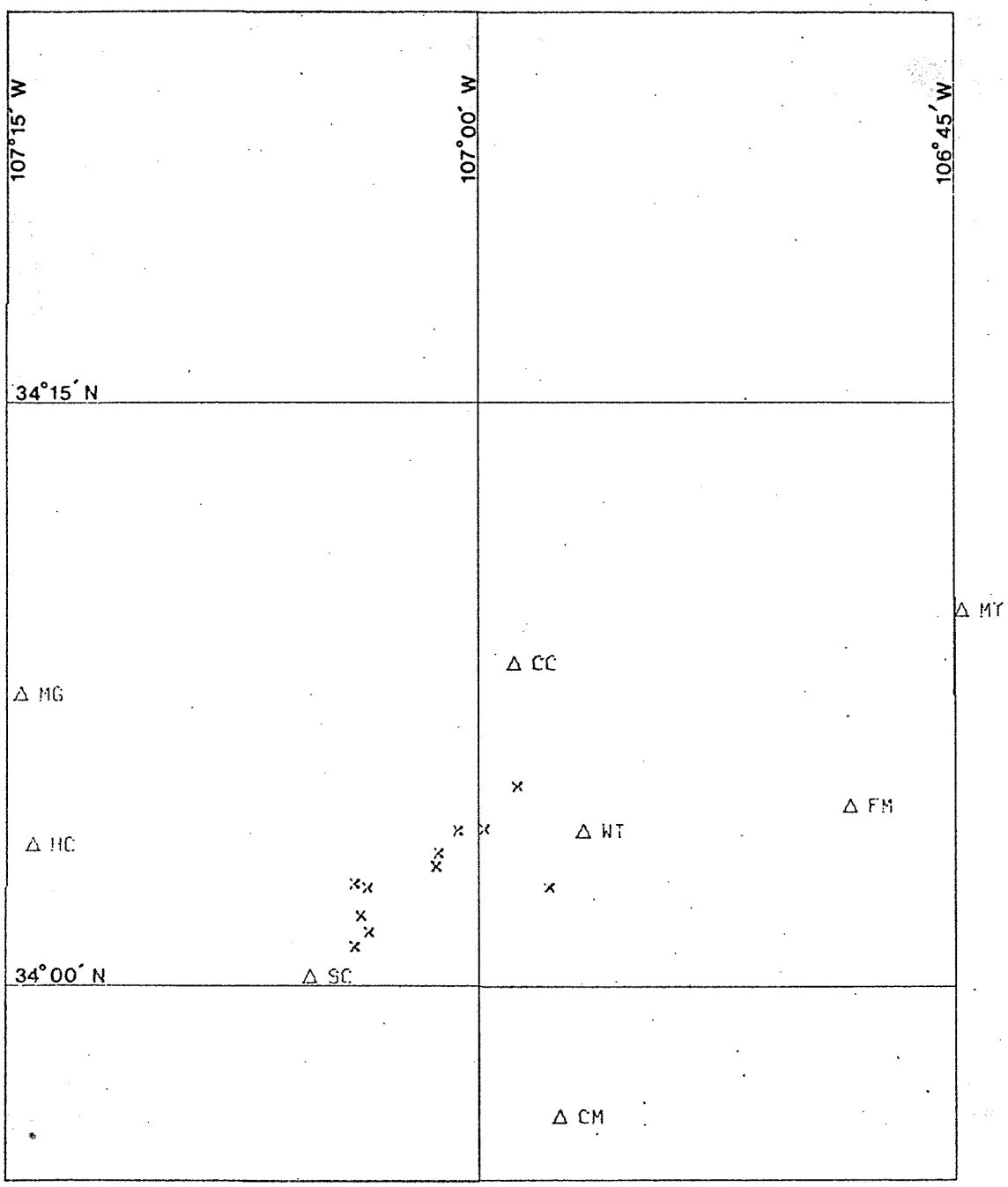

Figure 26. Map showing the S_XS points of reflection which indicate the magma layer occurs at greater than 21.0 km depth.

ACKNOWLEDGMENTS

The author wishes to sincerely thank Dr. Allan R. Sanford for his assistance in all facets of this research and to express his particular appreciation for Dr. Sanford's critical reveiw of this report. Thanks is also extended to Eric Rinehart and Paul Shuleski for their many hours spent in data acquistion and reduction. The author is also indebted to Leslie Rinehart for her patience while typing this report and to Dave Bollschweiler for his excellent drafting work. The author wishes to express particular appreciation to his wife for her constant encouragement and understanding.

REFERENCES CITED

Anderson, R. E. (1971). Thin skin distension in Tertiary rocks of southeastern Nevada, Geol. Soc. Amer. Bull. 82, 43-48.

Brown, D. M. (1972). Geology of the southern Bear Mountains, Socorro County, M. S. Thesis, New Mexico Inst. Mining Tech., Socorro, 110 p.

Bruning, J. E. (1973). Origin of the Popotosa formation, north-central Socorro County, New Mexico, Ph. D. Dissertation, New Mexico Inst. Mining Tech., Socorro, 132 p.

Burke, W. H., G. S. Kenny, J. B. Walker, and R. D. Walker (1963). Potassium-argon dates, Socorro and Sierra Counties, New Mexico, in New Mexico Geol. Soc. Guide book, 14th. Field Conf., 224.

Chapin, C. E. (1971). Rio Grande rift, Part I: Modifications and additions, in New Mexico Geol. Soc. Guidebook, 22nd. Field Conf., 59-71.

Chapin, C. E. and W. R. Seager (1975). Evolution of the Rio Grande rift in the Socorro and Las Cruces areas, in New Mexico Geol. Soc. Guidebook, 26th. Field Conf., 297-321.

Dane, C. H. and G. D. Bachman (1965). Geologic map of New Mexico, U. S. Geol. Survey, scale 1:500,00.

Denny, C. S. (1941). Quaternary geology of San Acacia area, New Mexico, Journal Geol. 49, 225-260.

Eaton, J. P. and K. J. Murata (1960). How volcanoes grow, Science 132, 925-938.

Gutenburg, B. (1941). Mechanism of faulting in Southern California indicated by seismograms, Bull. Seismol. Soc. Amer. 31, 263-302.

Hall, T. (1963). Springs in the vicinity of Socorro, New Mexico, in New Mexico Geol. Soc. Guidebook, 14th. Field Conf., 160-179.

Herber, L. J. (1962). Structural petrology and economic features of the Precambrian rocks of the La Joyita Hills, M. S. Thesis, New Mexico Inst. Mining Tech., Socorro, 36p.

Ramananantoandro, R. (1965). A magnetic survey of the southern Socorro Mountains, New Mexico, M. S. Thesis, New Mexico Inst. Mining Tech., Socorro, 38p.

Richter, C. F. (1958). Elementary Seismology, W. H. Freeman and Co., San Francisco.

Sanford, A. R. (1963). Seismic activity near Socorro, in New Mexico Geol. Soc. Guidebook, 14th. Field Conf., 146-151.

Sanford, A. R. (1968). Gravity survey in central Socorro County, New Mexico, Circ. 91, New Mexico State Bur. Mines Mineral Resources, 14p.

Sanford, A. R., O. Alptekin, and T. R. Toppozada (1973). Use of reflection phases on microearthquake seismograms to map an unusual discontinuity beneath the Rio Grande rift, Bull. Seismol. Soc. Amer. 63, 2021-2034.

Sanford, A. R., A. J. Budding, J. P. Hoffman, O. S. Alptekin, C. A. Rush, and T. R. Toppozada (1972). Seismicity of Rio Grande rift in New Mexico, Circ. 120, New Mexico State Bur. Mines Mineral Resources, 19p.

Sanford, A. R. and C. R. Holmes (1961). Note on the July 1960 earthquakes in central New Mexico, Bull. Seismol. Soc. Amer. 51, 311-314.

Sanford, A. R. and C. R. Holmes (1962). Microearthquakes near Socorro, New Mexico, Jour. of Geophys. Res. 67, 4449-4459.

Sanford, A. R. and L. T. Long (1965). Microearthquake crustal reflections, Bull. Seismol. Soc. Amer. 55, 579-586.

Sanford, A. R. and S. Singh (1968). Minimum recording times for determining short-term seismicity from microearthquake activity, Bull. Seismol. Soc. Amer. 58, 639-644.

Singh, S. (1970). Statistical analysis of microearthquakes of the Socorro region, Ph. D. Dissertation, New Mexico Inst. Mining Tech., Socorro, 156p.

Stuart, W. D. and J. S. Johnston (1975). Instrusive origin of the Matsushiro earthquake swarm, Geology 3, 63-67.

Summers, W. K. (1965). A preliminary report on New Mexico's geothermal energy resources, Circ. 80, New Mexico State Bur. Mines Mineral Resources, 41p.

Sukes, L. R. (1970). Earthquake swarms and sea floor spreading, Jour. of Geophys. Res. 75, 6598-6611.

Willard, M. E. (1971). K-Ar ages of the volcanic rocks in Luis Lopez manganese district, Socorro Co., New Mexico, Isochron/West 71-2, 47-48.

Woodward, T. M. (1973). Geology of the Lemitar Mountains, Socorro County, New Mexico, M. S. Thesis, New Mexico Inst. Mining Tech., Socorro, 73p.